Biochem. J. (2012) **448**, 189–200 (Printed in Great Britain) doi:10.1042/BJ20120339

multimedia online data

2-APB-potentiated channels amplify CatSper-induced Ca^{2+} signals in human sperm

Linda LEFIÈVRE*†, Katherine NASH‡, Steven MANSELL§, Sarah COSTELLO‡, Emma PUNT‡, Joao CORREIA†‡, Jennifer MORRIS‡, Jackson KIRKMAN-BROWN*†, Stuart M. WILSON§, Christopher L. R. BARRATT§ and Stephen PUBLICOVER‡[1]

*Medical School, University of Birmingham, Birmingham B15 2TT, U.K., †Birmingham Women's Hospital, Birmingham B15 2TG, U.K., ‡School of Biosciences, University of Birmingham, Birmingham B15 2TT, U.K., and §Division of Cardiovascular Medicine, Medical Research Institute, Ninewells Hospital University of Dundee, Dundee DD1 9SY, Scotland, U.K.

$Ca^{2+}{}_i$ signalling is pivotal to sperm function. Progesterone, the best-characterized agonist of human sperm $Ca^{2+}{}_i$ signalling, stimulates a biphasic $[Ca^{2+}]_i$ rise, comprising a transient and subsequent sustained phase. In accordance with recent reports that progesterone directly activates CatSper, the $[Ca^{2+}]_i$ transient was detectable in the anterior flagellum (where CatSper is expressed) 1–2 s before responses in the head and neck. Pre-treatment with 5 μM 2-APB (2-aminoethoxydiphenyl borate), which enhances activity of store-operated channel proteins (Orai) by facilitating interaction with their activator [STIM (stromal interaction molecule)] 'amplified' progesterone-induced $[Ca^{2+}]_i$ transients at the sperm neck/midpiece without modifying kinetics. The flagellar $[Ca^{2+}]_i$ response was unchanged. 2-APB (5 μM) also enhanced the sustained response in the midpiece, possibly reflecting mitochondrial Ca^{2+} accumulation downstream of the potentiated $[Ca^{2+}]_i$ transient. Pre-treatment with 50–100 μM 2-APB failed to potentiate the transient and suppressed sustained $[Ca^{2+}]_i$ elevation. When applied during the $[Ca^{2+}]_i$ plateau, 50–100 μM 2-APB caused a transient fall in $[Ca^{2+}]_i$, which then recovered despite the continued presence of 2-APB. Loperamide (a chemically different store-operated channel agonist) enhanced the progesterone-induced $[Ca^{2+}]_i$ signal and potentiated progesterone-induced hyperactivated motility. Neither 2-APB nor loperamide raised pH_i (which would activate CatSper) and both compounds inhibited CatSper currents. STIM and Orai were detected and localized primarily to the neck/midpiece and acrosome where Ca^{2+} stores are present and the effects of 2-APB are focussed, but store-operated currents could not be detected in human sperm. We propose that 2-APB-sensitive channels amplify $[Ca^{2+}]_i$ elevation induced by progesterone (and other CatSper agonists), amplifying, propagating and providing spatio-temporal complexity in $[Ca^{2+}]_i$ signals of human sperm.

Key words: calcium, CatSper, hyperactivation, progesterone, sperm, store-operated channel.

INTRODUCTION

Within the female tract, mammalian sperm receive essential 'cues' from the tract itself and from the cumulus–oocyte complex. These cues regulate a variety of the sperm's activities through Ca^{2+} signalling [1]. Although $[Ca^{2+}]_i$ signals in sperm are diverse and often complex [1], patch-clamp studies have, so far, detected only a handful of channels, and only one Ca^{2+}-permeable channel, the pH_i-regulated channel CatSper, which is expressed only in the sperm flagellum [2,3]. CatSper is sensitive to pH_i, E_m (membrane potential) and a range of small organic molecules, such that it can be viewed as a 'polymodal chemosensor'[4]. Thus sperm Ca^{2+} signals, even those in the head, may be mediated primarily or completely through CatSper [4,5].

Progesterone, which is present at high micromolar levels in the cumulus and at low concentrations throughout the tract, is by far the best characterized natural agonist of human sperm activity, modulating the crucial functions of motility and acrosome reaction [6]. These effects are exerted through Ca^{2+} influx, which generates a $[Ca^{2+}]_i$ transient followed by a prolonged plateau [7,8]. This $[Ca^{2+}]_i$ signal is correlated with fertility [9,10], illustrating the importance of progesterone [and/or the signalling process(es) that it activates] in sperm function. Consistent with a central role for CatSper channels in sperm $[Ca^{2+}]_i$ signalling, it has recently been shown that progesterone activates CatSper in human sperm [11,12]. A key question, therefore, is whether this CatSper-mediated Ca^{2+} entry is sufficient to explain fully progesterone-induced Ca^{2+} signalling in sperm and its crucial effects on sperm function.

Blackmore [13] and, more recently, Park et al. [14] proposed that CCE (capacitative Ca^{2+} entry), the process by which mobilization of stored Ca^{2+} induces Ca^{2+}-influx at the plasmalemma [15], may contribute to the action of progesterone. CCE requires both a membrane Ca^{2+}-permeable channel and a mechanism by which $[Ca^{2+}]$ in the store is monitored. In somatic cells, the protein STIM (stromal interaction molecule) situated in the endoplasmic reticulum membrane detects luminal $[Ca^{2+}]$. Upon store mobilization, STIM redistributes into 'puncta' adjacent to the plasma membrane, where it activates Ca^{2+}-permeable SOCs (store-operated channels) [16]. SOC proteins include the Orai family (also named CRACM) and possibly members of the TRPC (transient receptor potential canonical) family, which may form heterologous tetramers with Orai subunits [17–19].

Abbreviations used: 2-APB, 2-aminoethoxydiphenyl borate; BCECF, 2′,7′-bis-(2-carboxyethyl)-5(6)-carboxyfluorescein; CCD, charge-coupled-device; CCE, capacitative Ca^{2+} entry; DVF, divalent-free; GFP, green fluorescent protein; HEK, human embryonic kidney; IP_3R, inositol trisphosphate receptor; OGB, Oregon Green BAPTA; PHN, posterior head and neck; sEBSS, supplemented Earle's balanced salt solution; SERCA, sarcoplasmic/endoplasmic reticulum Ca^{2+}-ATPase; SOC, store-operated channel; STIM, stromal interaction molecule; TRPC, transient receptor potential canonical; TRPV3, transient receptor potential vanilloid 3.

[1] To whom correspondence should be addressed (email s.j.publicover@bham.ac.uk).

In cells transfected with STIM, low doses ($<10\ \mu$M) of 2-APB (2-aminoethoxydiphenyl borate) [20] potentiate CCE by promoting the interaction of STIM with SOCs and also regulating gating of the channel [21–23]. 2-APB can also activate some STIM–Orai complexes without store mobilization [24–26]. At higher concentrations ($\geqslant 50\ \mu$M), the drug inhibits CCE, although this effect is dependent on the isoform of Orai expressed [24,25,27,28]. 2-APB can affect other aspects of Ca^{2+} signalling [29,30] but these non-target effects occur at high doses {$\geqslant 100\ \mu$M; IC_{50} for inhibition of microsomal IP_3Rs (inositol trisphosphate receptors) = 220–1000 μM and IC_{50} for SERCA (sarcoplasmic/endoplasmic reticulum Ca^{2+}-ATPase) = 375–725 μM depending on isoform [31,32]}. In the present study we report that Ca^{2+} signalling activated by progesterone is amplified by low concentrations of 2-APB and by loperamide, another modulator of these channels. These effects are not exerted through CatSper and are localized to the sperm neck and midpiece where Ca^{2+} stores are present and where we detect expression of STIM and Orai proteins.

EXPERIMENTAL

Saline solutions

sEBSS (supplemented Earle's balanced salt solution) contained 1.0167 mM NaH_2PO_4, 5.4 mM KCl, 0.811 mM $MgSO_4 \cdot 7H_2O$, 5.5 mM $C_6H_{12}O_6$, 2.5 mM $C_3H_3NaO_3$, 19.0 mM $CH_3CH(OH)COONa$, 1.8 mM $CaCl_2 \cdot 2H_2O$, 25.0 mM $NaHCO_3$, 118.4 mM NaCl and 15 mM Hepes (pH 7.35, 285–295 mOsm), supplemented with 0.3 % fatty-acid-free BSA. In non-capacitating medium (bicarbonate-free sEBSS), $NaHCO_3$ was omitted and osmotic strength was maintained by adjusting NaCl. Low Ca^{2+} EGTA-buffered sEBSS ($\approx 3 \times 10^{-7}$ M Ca^{2+}) contained 5 mM Ca^{2+} and 6 mM EGTA.

Preparation and capacitation of spermatozoa

Donors were recruited in accordance with the Human and Embryology Authority Code of Practice (Version 7) and gave informed consent (University of Birmingham Life and Health Sciences ERC 07-009 and 08/S1402/6 from the Tayside Committee of Medical Research Ethics B). Cells were harvested by direct swim-up as described previously [33] and adjusted to 6×10^6 cells/ml. Aliquots of 200 μl were left to capacitate for 5–6 h.

For Western blotting analysis and immunoprecipitation, cells were separated from seminal plasma by densitometry using a two-layer Percoll gradient (40 and 80 %) as described previously [34] and were capacitated as described above.

Single-cell imaging of $[Ca^{2+}]_i$

Loading of cells with OGB {Oregon Green BAPTA [1,2-bis-(*o*-aminophenoxy)ethane-*N*,*N*,*N*′,*N*′-tetra-acetic acid] 1} and time-lapse fluorescence imaging was as described previously [33]. All experiments were performed at 25 ± 0.5 °C in a continuous flow of medium {sEBSS or EGTA-buffered saline ($[Ca^{2+}]_o \approx 3 \times 10^{-7}$ M)}. Images were captured at 0.1 Hz (except where stated otherwise) using a 40× oil-immersion objective and a Q Imaging Rolera-XR cooled CCD (charge-coupled-device) camera or a Andor Ixon 897 EMCCD (electron-multiplying CCD) camera controlled by iQ software (Andor Technology).

Analysis of images, background correction and normalization of data was performed as described previously [33]. Unless stated otherwise, the region of interest was drawn around the PHN (posterior head and neck) region of each cell. Raw intensity values were imported into Microsoft Excel and normalized using the equation:

$$\Delta F = [(F - F_{rest})/F_{rest}] \times 100\ \%$$

where ΔF is the percentage change in fluorescence intensity at time t, F is fluorescence intensity at time t and F_{rest} is the mean of $\geqslant 10$ determinations of F during the control period. To compare the responses between experiments, we calculated ΔF_{mean}, the mean ΔF of all the cells ($n = 50$–200) in the experiment.

The amplitude of the progesterone-induced $[Ca^{2+}]_i$ transient was calculated from the three points spanning the peak of the ΔF_{mean} trace. Plateau amplitude was calculated from three consecutive points 4 min after application of progesterone. In experiments involving pre-treatment with 2-APB or loperamide transient peak and plateau values were corrected for ΔF (or ΔF_{mean}) immediately before progesterone application (Supplementary Figure S1 at http://www.BiochemJ.org/bj/448/bj4480189add.htm).

Population fluorimetry

$[Ca^{2+}]_i$ assessment was as described previously [35]. For assessment of pH_i, 2 ml aliquots were labelled with 1 μM BCECF-AM [2′,7′-bis-(2-carboxyethyl)-5(6)-carboxyfluorescein acetoxymethyl ester; 30 min, 37 °C, 5 % CO_2], centrifuged (300 ***g***, 5 min) then resuspended in sEBSS. Sampling rate was 12.5 Hz using excitation 440/495 nm and emission 535 nm. pH_i was calibrated similarly to [36].

Patch-clamp

Whole-cell currents were evoked by 1 s voltage ramps from − 80 mV to + 80 mV from a holding potential of 0 mV (before correction for junction potential). DVF (divalent-free) medium for recording CatSper currents contained 140 mM caesium methanesulfonate, 40 mM Hepes and 1 mM EGTA, pH 7.4, as described by Lishko et al. [11]. The pipette saline contained 130 mM caesium methanesulfonate, 70 mM Hepes, 3 mM EGTA, 2 mM EDTA and 0.5 mM Tris/HCl, pH 7.4.

Detection of proteins by Western blotting

Sperm proteins were extracted using RIPA buffer [150 mM NaCl, 20 mM Tris/HCl, pH 7.4, 2 mM DTT (dithiothreitol) and 1 % Triton X-100] supplemented with 0.5 % SDS and Complete™ protease inhibitor cocktail (Roche). Following brief sonication (MSE Soniprep 150, 20 s at 20 °C), samples were incubated for 30 min at 4 °C then centrifuged at 18 000 ***g*** for 15 min at 4 °C to remove any insoluble material. Aliquots of supernatant (20 μl) were kept for SDS/PAGE.

Electrophoresis was performed as described previously [37]. Proteins were separated by SDS/PAGE using 10 % gels for STIM and 15 % gels for Orai. Membranes were incubated overnight (4 °C) with the respective anti-Orai (1:250 dilution, ProSci; or 1:200 dilution, Sigma) or anti-STIM (1:1000 dilution, ProSci) antibodies. Where possible, pre-adsorption of antibodies with their corresponding antigenic peptides was carried out to assess the specificity of the detection. Antibody (1 μg) was pre-adsorbed with excess (1 μg) peptide for 1 h at room temperature (20 °C). Incubations with peptide-pre-adsorbed and non-pre-adsorbed antibodies were performed in parallel.

Immunoprecipitation

Percoll-washed spermatozoa (at least 200×10^6 cells per condition) were solubilized using RIPA buffer supplemented with 0.5 % SDS and Complete™ protease inhibitor cocktail. Following brief sonication, samples were incubated at 4 °C for 1 h then diluted 10-fold with RIPA buffer to avoid SDS interference with immunoprecipitation procedures. Samples were centrifuged at 18 000 ***g*** (15 min, 4 °C) to remove insoluble material. A pre-clearing step involved incubation with 30 μl of a pre-washed Protein G plus/Protein A–agarose beads (33 % slurry suspension; Calbiochem) for 30 min at 4 °C followed by a centrifugation at 2500 ***g*** (5 min). Pre-cleared sperm lysate was further centrifuged (13 000 ***g***, 10 min) and the supernatant was transferred to a fresh microfuge tube and kept at 4 °C.

Protein G plus/Protein A–agarose beads (20 μl) (33 % slurry suspension) were incubated overnight with 1 μg of antibody in 750 μl of RIPA buffer then washed three times with RIPA buffer and the remaining supernatant was aspirated away. Pre-cleared sperm lysate was then added to the antibody-coated beads and incubated for 90 min (4 °C). The immunocomplex was pelleted by centrifugation (2500 ***g***, 5 min) and washed three times with 1 ml of immunoprecipitation buffer followed by twice with 1 ml of PBS. The immunoprecipitated proteins were resuspended in 20 μl of 1× SDS sample buffer, incubated at 70 °C for 10 min and submitted to SDS/PAGE as described above.

Detection of Orai and STIM by immunofluorescence

Percoll-washed spermatozoa (2×10^5 cells) were prepared for immunocytochemistry as described in [35]. Slides were incubated overnight (4 °C) with anti-Orai (1:10 dilution, ProSci and Sigma) and anti-STIM antibodies (1:25 dilution, ProSci). Where possible, pre-adsorption of Orai and STIM antibodies with their corresponding antigenic peptides was carried out (as described above) to assess specificity. Experiments using peptide-pre-adsorbed and non-pre-adsorbed antibodies were performed in parallel. Slides were then prepared as described in [35].

Assessment of distribution of STIM

After capacitation as described above or immediately after swim-up into non-capacitating sEBSS, 200 μl aliquots of spermatozoa were exposed to bis-phenol (15 μM). After 12 min, cells were centrifuged (2000 ***g***, 5 min) then fixed in 4 % formaldehyde (6 min). Cells were re-centrifuged, resuspended in PBS, smeared on poly-L-lysine-coated slides and air-dried. Permeabilization, antibody staining and processing for assessment of acrosome reaction were as described above.

Statistical analysis

Values given in the text are means ± S.E.M. For most comparisons we used ΔF_{mean} values obtained from parallel control and pre-treatment experiments such that '*n*' refers to the number of pairs of experiments. Each ΔF_{mean} value was the average of 50–200 normalized single-cell responses. Microsoft Excel was used to calculate correlation coefficients and perform paired or unpaired *t* tests and χ^2 tests as appropriate. Where *n* is the number of cells this is stated.

RESULTS AND DISCUSSION

Effect of 2-APB on resting $[Ca^{2+}]_i$ in human sperm

Treatment of sperm with 5 μM 2-APB increased $[Ca^{2+}]_i$ in ~75 % of cells, inducing a plateau or a series of transients

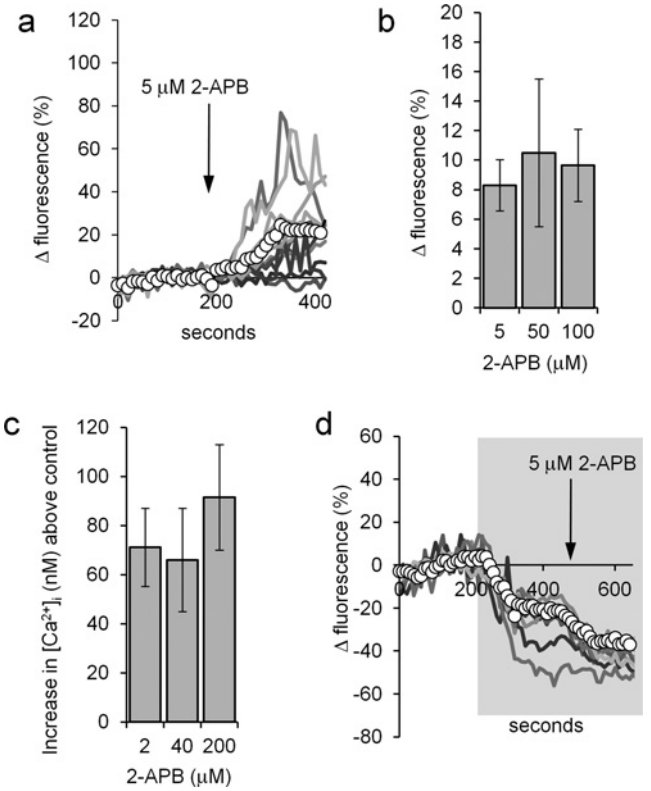

Figure 1 2-APB elevates resting $[Ca^{2+}]_i$

(**a**) 2-APB (5 μM; arrow) causes a sustained increase in the PHN $[Ca^{2+}]_i$ of a subset of cells. The traces show ten individual cell responses and ΔF_{mean} (○-○) for all 87 cells in the experiment. (**b** and **c**) 2-APB-induced $[Ca^{2+}]_i$ elevation is dose-independent. (**b**) Increase in ΔF_{mean} 3 min after application of 2-APB. Results are means ± S.E.M. for sets of four experiments in each of which aliquots from the sample were tested with each of the three concentrations of 2-APB. (**c**) Dose-dependence of 2-APB-induced $[Ca^{2+}]_i$ increment in fura-2-loaded cell populations (means ± S.E.M. for 6–17 experiments). (**d**) 2-APB-induced rise in $[Ca^{2+}]_i$ is reversed in low-Ca^{2+} saline. Cells were superfused with EGTA-buffered saline (shown by shading) then exposed to 5 μM 2-APB (arrow). 2-APB-induced $[Ca^{2+}]_i$ increase was abolished and in many cells 2-APB induced a further fall in $[Ca^{2+}]_i$. Traces show six individual cell responses and ΔF_{mean} (○-○) for all 85 cells in the experiment.

(Figure 1a). Within ~100 s, ΔF_{mean} stabilized at an increased level and at 3 min was 15.6 ± 3.7 % at the PHN and 8.5 ± 2.9 % at the midpiece ($P = 0.008$; paired *t* test, $n = 11$ experiments). Higher doses of 2-APB (up to 100 μM) had similar effects to 5 μM (Figure 1b; $P > 0.5$; paired *t* test, $n = 4$) and the same dose-insensitivity was observed when $[Ca^{2+}]_i$ was measured in fura-2-loaded cell populations (Figure 1c). When cells were prepared under non-capacitating conditions (BSA and bicarbonate-free sEBSS but containing Ca^{2+}), the increase in resting $[Ca^{2+}]_i$ induced by 5 μM 2-APB was significantly smaller (PHN ΔF_{mean} at 3 min = 7.4 ± 2.0 %; $n = 7$; $P = 0.03$).

Superfusion of capacitated cells with EGTA-buffered medium (~3×10^{-7}M Ca^{2+}) for 3 min prior to the application of 5 μM 2-APB caused a sustained fall in $[Ca^{2+}]_i$ and abolished the stimulatory effect of 2-APB, showing that the drug was not releasing stored Ca^{2+}. In addition, in more than 20 % of cells (22 ± 3 %; $n = 5$) application of 2-APB induced a further $[Ca^{2+}]_i$ decrease, which was visible as a fall in ΔF_{mean} (Figure 1d). Similar effects were seen with 50 and 100 μM 2-APB. This reversal of the effect of 2-APB upon buffering of $[Ca^{2+}]_o$ shows that it acts by increasing plasma membrane Ca^{2+} permeability.

2-APB might increase membrane Ca^{2+} flux by activating CatSper either directly [4] or by cytoplasmic alkalinization [11].

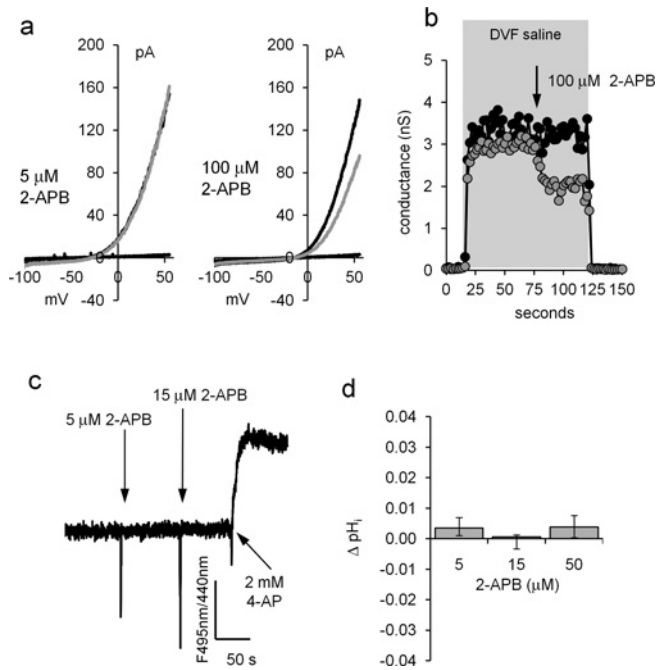

Figure 2 2-APB does not enhance CatSper currents

(**a**) Monovalent CatSper currents recorded before (black trace) and after (grey trace) application of 5 μM (left-hand panel) and 100 μM (right-hand panel) 2-APB. Horizontal (near zero) traces show currents in divalent cation-containing saline. (**b**) Time course of CatSper current block by 100 μM 2-APB. Cell conductance was calculated from the slope between + 50 and + 60 mV. Grey shading shows superfusion with DVF saline, arrow shows application of 2-APB. (**c**) 2-APB does not raise pH_i. 2-APB at 5 and 15 μM was added at the first and second arrows respectively. 4-Aminopyridine (2 mM; 4-AP; positive control) caused an immediate rise in pH_i. (**d**) Mean pH_i change ($\pm$S.E.M.) in response to 5 μM ($n=6$), 15 μM ($n=3$) and 50 μM ($n=3$) 2-APB.

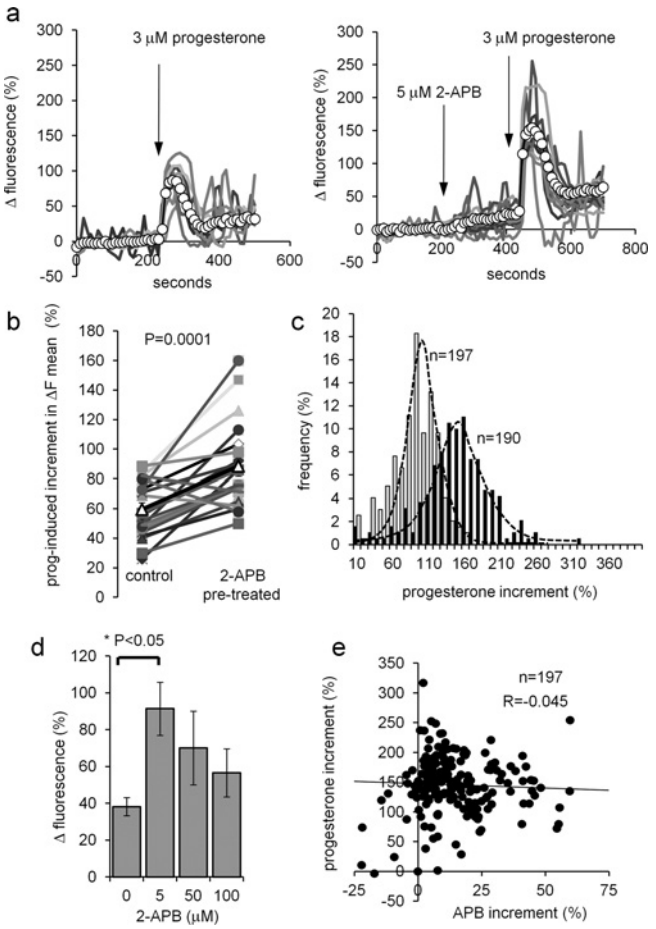

Figure 3 2-APB modulates the progesterone-induced $[Ca^{2+}]_i$ transient

(**a**) Elevation of $[Ca^{2+}]_i$ at the PHN in response to stimulation with 3 μM progesterone (arrow) under control conditions (left-hand panel) and after 200 s exposure to 5 μM 2-APB (right-hand panel). Both experiments used cells from the same preparation. Traces show 6–8 representative single-cell responses and ΔF_{mean} (○-○) for all 107 (left-hand panel) and 125 (right-hand panel) cells in the experiment. (**b**) Summary of results from 20 pairs of control and 5 μM 2-APB-pre-treated experiments. Each point shows the mean amplitude of the progesterone-induced transient (increment in ΔF_{mean}) for all of the cells in a single experiment (50–200 cells). Joined pairs of points show 5 μM 2-APB pre-treatment (right-hand point) and corresponding control (left-hand point) using cells from the same ejaculate – such as the pair shown in (**a**). Data from 20 pairs of experiments are shown and the overall mean for all 20 is shown by Δ-Δ. (**c**) Effect of 5 μM 2-APB on amplitude distribution of single-cell progesterone-induced transients. Grey bars show the control, black bars show the parallel 5 μM 2-APB-pre-treated experiment. (**d**) Dose-dependence of potentiation by 2-APB of the progesterone-induced $[Ca^{2+}]_i$ transient. Each bar shows the mean amplitude $\pm$ S.E.M. for four sets of experiments (50–200 cells each). In each set, four experiments were carried out with samples from the same ejaculate, using 0, 5, 50 or 100 μM 2-APB applied 200 s before progesterone. Only 5 μM 2-APB significantly enhanced the $[Ca^{2+}]_i$ transient. (**e**) Amplitude of 2-APB-induced resting $[Ca^{2+}]_i$ elevation (APB increment; *x*-axis) is not correlated with the amplitude of subsequent progesterone-induced $[Ca^{2+}]_i$ transient (progesterone increment; *y*-axis). Results are from 197 cells in one experiment.

When human sperm monovalent CatSper currents were measured by whole-cell patch-clamping, the I–V curve showed a virtual absence of inward current, as described by Lishko et al. [11] using the same recording conditions. 2-APB (5 μM) had no effect on the large outward current (measured at + 55 mV; $P > 0.4$, $n=6$), but at 100 μM the current was inhibited by 43 ± 4 % ($P < 0.0002$; $n=8$; Figures 2a and 2b). We assessed the effect of 2-APB on pH_i using BCECF. Concentrations of 2-APB at 5, 15 and 50 μM increased pH_i by 0.003 ± 0.002, 0.001 ± 0.004 and 0.004 ± 0.003 respectively (not significant, $n=3$; Figures 2c and 2d). In the absence of store mobilization, 2-APB dose-independently activates a plasma membrane Ca^{2+}-permeable channel in human sperm that is not CatSper. 2-APB, at doses from 2 to 100 μM, has been shown to activate Ca^{2+} influx and SOC currents without mobilization of stored Ca^{2+} in cells expressing Orai 3 (where a change in pore characteristics occurred) [24,25] and also in cells co-expressing Orai with STIM2 [26].

2-APB enhances the progesterone-induced $[Ca^{2+}]_i$ transient

The non-genomic action of progesterone on $[Ca^{2+}]_i$ in human sperm has a biphasic dose–effect relationship, apparently reflecting effects at high- and low-affinity receptors [12,38]. Experiments were carried out using 3 μM progesterone because: (i) this dose reflects concentrations in follicular fluid and the cumulus oophorous [39]; and (ii) in our previous imaging and fluorimetric studies, this concentration fully saturated the high-affinity $[Ca^{2+}]_i$ response but did not recruit a low-affinity receptor response [40]. The latter is important, since exceeding the saturating dose will both minimize effects of any variation in the concentration profile occurring during progesterone application and reduce any effects of 2-APB on the affinity of progesterone for its receptor. These effects could profoundly affect the responses to sub-saturating concentrations of progesterone.

$[Ca^{2+}]_i$ in PHN

In PHN, 3 μM progesterone induced a transient increase in $[Ca^{2+}]_i$ followed by a plateau in >90 % of cells that was clearly visible in the ΔF_{mean} trace (Figure 3a, ○-○) [41]. To test the

effect of 2-APB on this response, experiments were carried out in pairs, where cells from the same semen sample were exposed to 3 μM progesterone with and without 2-APB pre-treatment. In 17 out of 20 experiment pairs, pre-treatment with 5 μM 2-APB (200 s) enhanced the amplitude of the progesterone-induced increment in ΔF_{mean} (pre-treated/control ratio $= 1.58 \pm 0.13$, $n = 20$; $P = 0.0001$, paired t test; Figures 3a and 3b). Population (fluorimetric) recordings from fura-2-loaded cells confirmed this observation, 2 μM 2-APB increasing the amplitude of the $[Ca^{2+}]_i$ transient from 137 ± 28 nM to 289 ± 42 nM ($P = 0.0005$; $n = 14$). These effects occurred at doses >50× lower than the reported IC_{50} values for inhibition of SERCAs or IP_3Rs [31,32]. That this potentiating action was not associated with the effects of 2-APB on Ca^{2+} clearance mechanisms was confirmed by analysis of the decay kinetics of progesterone-induced $[Ca^{2+}]_i$ transients. Inhibition of Ca^{2+} ATPases with bis-phenol (which does not increase the progesterone transient amplitude in human sperm) slows Ca^{2+} clearance, extending decay duration 2–3-fold [42,43]. In contrast, pre-treatment with 2-APB extended decay duration (from ΔF_{mean} peak to inflexion at the end of falling phase) by only 11 % (from 107 ± 7 s to 119 ± 7 s; $P = 0.03$; paired t test, $n = 16$) and the absolute rate of decay was increased from 0.80 ± 0.09 to 1.16 ± 0.10 % per second ($P < 0.02$; paired t test, $n = 16$ experimental pairs), consistent with stimulation of Ca^{2+} clearance at increased $[Ca^{2+}]_i$.

In eight experiment pairs where the effect of 5 μM pre-treatment was large, we compared the amplitude distributions of single-cell $[Ca^{2+}]_i$ transients in control and 2-APB-pre-treated cells. The distribution was bell-shaped under control conditions, and in five out of the eight experiments, 5 μM 2-APB simply shifted this distribution along the axis, only 5–10 % of cells generating $[Ca^{2+}]_i$ transients of amplitude similar to the parallel control (Figure 3c). In the three other experiments the 2-APB pre-treatment resulted in a bi-modal or 'smeared' amplitude distribution (Supplementary Figure S2 at http://www.BiochemJ.org/bj/448/bj4480189add.htm).

Pre-treatment with 50 μM or 100 μM 2-APB enhanced $[Ca^{2+}]_i$ transient amplitude in some experiments (Supplementary Figure S3 at http://www.BiochemJ.org/bj/448/bj4480189add.htm and Figure 3d), but this effect was not significant ($P > 0.2$; paired t test, $n = 4$ sets of experiments). There was a clear difference in dose-dependence between the effects of 2-APB on resting $[Ca^{2+}]_i$ and on progesterone-induced signalling (compare Figures 1b and 1c with Figure 3d).

The amplitude of the progesterone-induced $[Ca^{2+}]_i$ signal in human sperm is capacitation-dependent [44]. We therefore investigated the effect of 5 μM 2-APB pre-treatment on cells prepared in the absence of bicarbonate and BSA (non-capacitating conditions). The $[Ca^{2+}]_i$ transient in these experiments was reduced compared with 'capacitated' cells ($\Delta F_{mean} = 37.6 \pm 7.1$ %, $n = 7$ experiments and 59.6 ± 4.5 %, $n = 20$ experiments respectively; $P < 0.025$), but pre-treatment with 5 μM 2-APB was still effective, enhancing transient amplitude (82 ± 30 %; $P = 0.017$; $n = 7$ experimental pairs; paired t test), an effect similar to that in cells prepared in capacitating medium ($P = 0.39$).

In experiments where 5 μM 2-APB pre-treatment caused marked elevation of resting $[Ca^{2+}]_i$, we analysed the relationship between this effect and the amplitude of the response (in the same cell) to subsequent application of progesterone ('e' and 'c' in Supplementary Figure S1). There was no correlation (Figure 3e; $R = 0.10 \pm 0.08$; $n = 10$ experiments). 2-APB has two discrete effects, potentiating progesterone-induced Ca^{2+} influx at low micromolar doses and also increasing resting Ca^{2+} influx.

$[Ca^{2+}]_i$ responses in the flagellum

In OGB-loaded human sperm, fluorescence is most intense at the PHN. This probably reflects the presence of the cytoplasmic droplet in this region and it is likely that the signal from this region also dominates fluorimetric population recordings. However, the initial site of action of progesterone on human sperm is likely to be CatSper channels in the principal piece of the flagellum [11,12]. We therefore compared the effects of 2-APB pre-treatment on progesterone-stimulated $[Ca^{2+}]_i$ responses in the PHN with those in the flagellum.

Midpiece. In control experiments, application of progesterone caused a transient rise in $[Ca^{2+}]_i$ in the midpiece resembling that occurring at the PHN. Kinetics of rise and decay of ΔF_{mean} were similar ($P > 0.05$; $n = 11$ pairs of experiments). Transient amplitudes in the two regions were correlated ($R = 0.74$; Supplementary Figure S4 at http://www.BiochemJ.org/bj/448/bj4480189add.htm), but ΔF_{mean} at the peak was ~25 % smaller in the midpiece ($P < 0.002$; $n = 11$ pairs of experiments). After pre-treatment with 5 μM 2-APB, this relationship was maintained, but midpiece response amplitudes were supplemented by the recruitment of an extra 'late' component (Supplementary Figure S4; see below).

Principal piece. In five pairs of experiments (control and 5 μM 2-APB pre-treatment) we measured the progesterone-induced $[Ca^{2+}]_i$ signal in the anterior flagellar principal piece, using only cells where this could be reliably assessed (visible and in focus throughout experiment). Duration of the $[Ca^{2+}]_i$ transient in the principal piece was short, 74 ± 8 s compared with 143 ± 8 s in the PHN of the same cells ($P < 0.0005$), but the amplitude (normalized to pre-stimulus fluorescence) was significantly larger ($P = 0.0004$; $n = 43$ cells; Figure 4a). 2-APB pre-treatment enhanced the $[Ca^{2+}]_i$ transient recorded at the PHN (compared with controls), but at the principal piece we detected no effect of 2-APB (Figure 4b), such that the ratio of transient amplitude at the PHN/transient amplitude at the principal piece (in the same cell) increased from 0.8 ± 0.1 in control cells to 1.5 ± 0.2 in cells pre-treated with 5 μM 2-APB ($n = 43$ and $n = 57$ cells respectively; $P = 0.00011$; Figure 4c). We also assessed the effect of 2-APB on progesterone-potentiated CatSper currents. As reported previously [11,12], progesterone increased monovalent CatSper currents, particularly enhancing inward current (Figure 4d). 2-APB (5 μM) reduced CatSper current amplitude in four out of four experiments, inhibiting inward and outward currents by 21 ± 2 % ($P < 0.02$) and 16 ± 6 % ($P = 0.12$) respectively. 2-APB (100 μM) inhibited inward and outward currents by 68 ± 2 % ($P = 0.001$) and 72 ± 3 % ($P = 00003$) respectively ($n = 6$) (Figure 4d).

Thus 5 μM 2-APB enhances the progesterone-induced $[Ca^{2+}]_i$ transient in the PHN and midpiece but does not enhance CatSper-mediated Ca^{2+}-influx. Surprisingly, although 100 μM 2-APB significantly inhibited monovalent CatSper currents (Figures 2a, 2b and 4d), it failed to reduce the $[Ca^{2+}]_i$ transient amplitude (Figure 3d). One possible explanation is that high-dose 2-APB potentiates Ca^{2+} influx similarly to 5 μM 2-APB [24,25,27,28] and 'compensates' a smaller contribution from CatSper. In fact, since the kinetics of the 2-APB-enhanced response closely resemble those of the control response (mean time to peak being identical; $P = 0.5$; $n = 16$ pairs of experiments), 2-APB-sensitive channels may dominate the $[Ca^{2+}]_i$ signal recorded at the PHN.

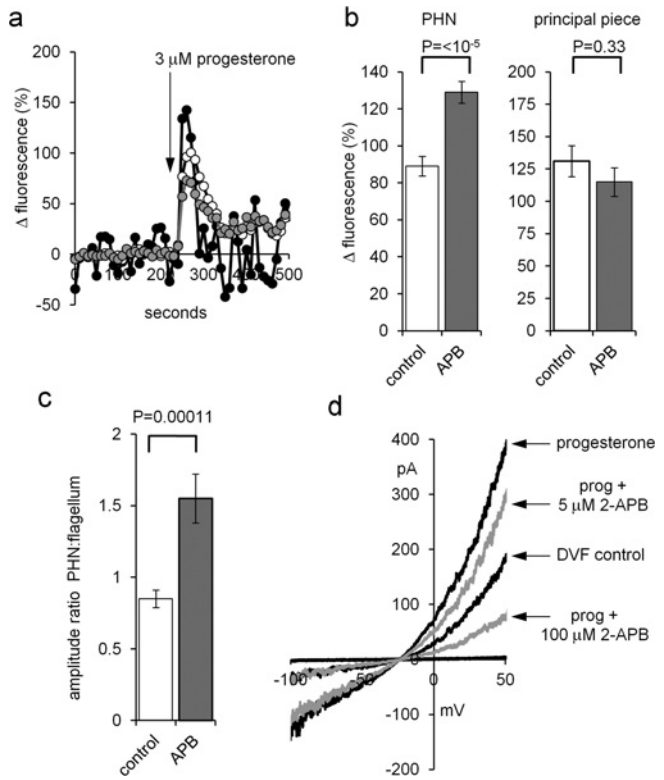

Figure 4 2-APB does not enhance the flagellar Ca^{2+} signal or potentiate activation of CatSper by progesterone

(**a**) $[Ca^{2+}]_i$ (OGB) signal from the PHN (white circles), midpiece (grey circles) and flagellum (black circles) in response to application of 3 μM progesterone (arrow). Each trace shows the mean response from the same nine cells. (**b**) Amplitude of progesterone-induced $[Ca^{2+}]_i$ transient at the PHN (left-hand panel) and midpiece (right-hand panel) under control conditions (white bars; $n = 43$ cells) and after pre-treatment with 5 μM 2-APB (grey bars; $n = 57$ cells). (**c**) Ratio of $[Ca^{2+}]_i$ transient amplitudes simultaneously recorded from the PHN and flagellum under control conditions (white bar; $n = 43$) and after pre-treatment with 5 μM 2-APB (grey bar; $n = 57$). (**d**) Monovalent currents (DVF control) were enhanced by 500 nM progesterone (upper black trace). Subsequent application of 5 μM 2-APB (upper grey trace) and 100 mM 2-APB (lower grey trace) reduced the amplitude of outward and inward currents.

Effects of 2-APB on the progesterone-induced sustained $[Ca^{2+}]_i$ elevation

Following the progesterone-induced $[Ca^{2+}]_i$ transient, there is a sustained elevation of $[Ca^{2+}]_i$ above resting levels. To assess the effect of 2-APB pretreatment on this $[Ca^{2+}]_i$ plateau, we used the value of ΔF_{mean} recorded 4 min after progesterone application ('b' and 'd' in Supplementary Figure S1). After 2-APB pretreatment, sustained $[Ca^{2+}]_i$ elevation at the PHN sometimes exceeded that in the parallel control (Figure 3a), but this effect was inconsistent and not significant (ΔF_{mean} at 240 s: control $= 19 \pm 2$ %; 2-APB pre-treated $= 20 \pm 3$ %; $P = 0.75$; paired t test; $n = 19$ pairs of experiments).

Recently, Park et al. [14] reported that progesterone-induced sustained $[Ca^{2+}]_i$ elevation was localized to the midpiece. In 11 of the experiment pairs (482 cells) we were able to analyse $[Ca^{2+}]_i$ at both the PHN and midpiece. As described above, the sustained $[Ca^{2+}]_i$ response (ΔF_{mean} 240 s after progesterone application) at the PHN showed no effect of pretreatment with 5 μM 2-APB (control $= 18 \pm 5$ %; 2-APB $= 20 \pm 6$ %; $P = 0.66$; $n = 11$ experiment pairs). However, in the same cells, the sustained increase in fluorescence at the midpiece was enhanced >3-fold, from 16 ± 4 % (control) to 52 ± 12 % (2-APB pre-treated; $P = 0.002$; $n = 11$ experiment pairs; Figures 5a–5c). The amplitude distribution of these 2-APB-enhanced sustained midpiece responses was bimodal (Figures 5b and 5d). When cells were pre-treated with 100 μM 2-APB, ΔF_{mean} recorded at the midpiece 240 s after progesterone was significantly smaller than in parallel controls ($P < 0.05$, $n = 6$ experimental pairs; $P < 0.005$; Figure 5c).

Late activation of the midpiece sustained responses

The rising phase of the progesterone-induced $[Ca^{2+}]_i$ increase in the midpiece of 2-APB-pre-treated cells often showed an inflexion, apparently reflecting a second 'delayed' rise in fluorescence occurring 20–30 s after stimulation (Figure 5e, black trace; arrowhead). In six pairs of experiments where the midpieces were well-immobilized we assessed the occurrence of this 'late' response. Approximately one-third of 5 μM 2-APB pre-treated cells (34 ± 6 %; 424 cells in six experiments) showed a clear inflexion, but this pattern of response was rare in parallel controls (7.6 ± 2.8 %; $n = 443$ cells in six experiments; $P = 0.01$; paired t test). This 'late' rise in fluorescence at the midpiece was always followed by a large (>80 % at 240 s; see Figure 5d) sustained increase in midpiece fluorescence. Association of these two events was highly non-random ($P = 10^{-10}$; χ^2 test). Thus it appears that the large type of sustained responses observed in the midpiece activates during the rising phase of the $[Ca^{2+}]_i$ transient, adding a 'step' to the signal. In three experiments we followed the kinetics of the response to progesterone in more detail by using an increased camera frame rate (10 Hz). Consistent with recent reports that progesterone directly activates CatSper channels [11,12], the $[Ca^{2+}]_i$ response in the anterior principal piece preceded that in the PHN region by 1.6 ± 0.2 s ($n = 29$ cells; $P < 10^{-8}$) (Figure 5f). A similar spatio-temporal pattern has recently been reported upon photolysis of caged progesterone [45]. When a sustained $[Ca^{2+}]_i$ increase occurred in the midpiece there was often a clear inflexion in the rising phase after 10–30 s (Figures 5f and 5g; Supplementary Movies S1 and S2 at http://www.BiochemJ.org/bj/448/bj4480189add.htm).

The sperm midpiece contains the sperm's mitochondria. Since the large 2-APB-potentiated sustained response is localized here and occurs 20–30 s after initiation of the $[Ca^{2+}]_i$ transient, it is likely that it includes a contribution from OGB within the mitochondrial matrix compartment, which will fluoresce upon mitochondrial Ca^{2+} accumulation. Imaging data do not allow us to distinguish confidently between mitochondrial Ca^{2+} accumulation and a discrete 'late' Ca^{2+} influx at the midpiece, but it may be significant that 5 μM 2-APB is reported to slow the export of Ca^{2+} from mitochondria [46]. Since Ca^{2+} uptake by mitochondria is by a low-affinity transporter [47], if this late response reflects mitochondrial Ca^{2+} accumulation it reveals a large increase in $[Ca^{2+}]_i$ in the midpiece of these sperm.

Application of 2-APB during the sustained component of the progesterone-induced $[Ca^{2+}]_i$ increase

To investigate further the effects of 2-APB on the sustained $[Ca^{2+}]_i$ increase, we applied the drug 6–7 min after progesterone stimulation, following completion of the $[Ca^{2+}]_i$ transient. 2-APB at 5 μM caused a reversible tonic increase in fluorescence at the PHN (21 ± 6 % increase in ΔF_{mean} at 4 min after application, four experiments; Figure 6a). The midpiece did not show the large sustained response that occurred when 2-APB was applied prior to progesterone. When 50 μM 2-APB was applied in this way there was an immediate but transient fall in $[Ca^{2+}]_i$. The $[Ca^{2+}]_i$ plateau ('b' in Supplementary Figure S1) was reduced by 62 ± 13 %

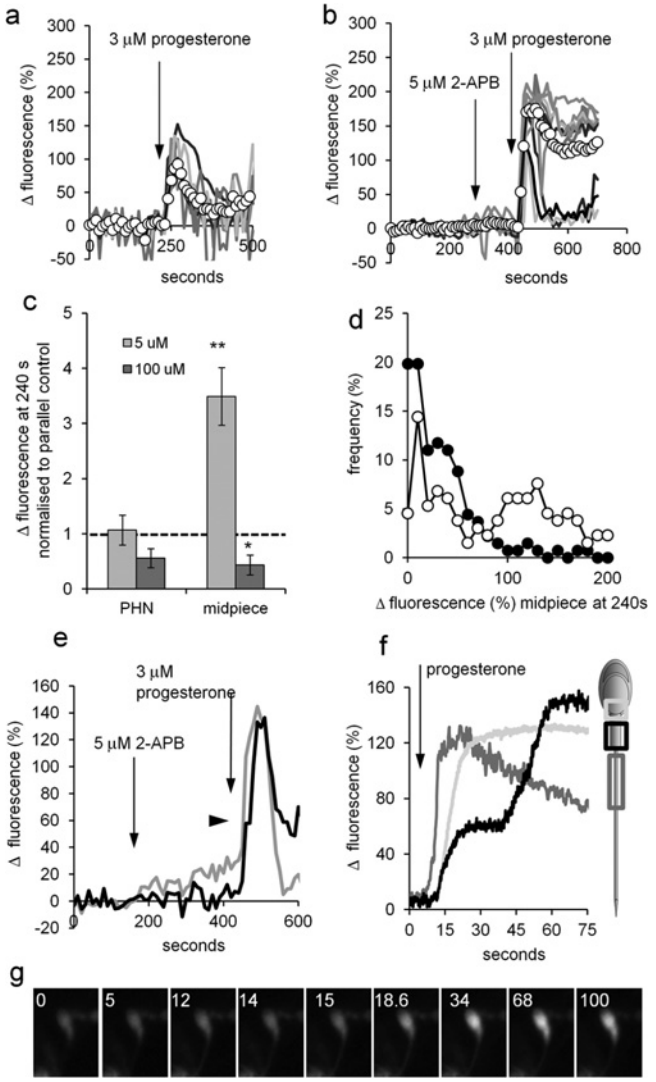

Figure 5 2-APB (5 μM) enhances sustained elevation of $[Ca^{2+}]_i$ in the midpiece

(**a** and **b**) Progesterone-induced responses at the midpiece under control conditions (**a**) and after application of 5 μM 2-APB (first arrow; **b**). Each plot shows six to nine representative single-cell traces and ΔF_{mean} (○-○) for all 25 (**a**) and 31 (**b**) cells in the experiment. (**c**) Dose-dependence of the effect of 2-APB pre-treatment on the sustained $[Ca^{2+}]_i$ signal. The amplitude of the sustained response (240 s after progesterone addition) in PHN (left-hand bars) and midpiece (right-hand bars) after exposure to 5 μM 2-APB (light grey bars) and 100 μM 2-APB (dark grey bars) was normalized to the amplitude of the parallel control (shown by a broken line). Each bar shows the means ± S.E.M. of 11 (5 μM 2-APB) and six (100 μM 2-APB) experiments. $*P < 0.05$; $**P < 0.005$ compared with control. (**d**) Amplitude distribution of single-cell sustained $[Ca^{2+}]_i$ increases (240 s after progesterone addition). Open circles (○-○) show responses of 2-APB pre-treated cells (136 cells from five experiments), closed circles (●-●) show responses from 135 cells in the five parallel control experiments. (**e**) Progesterone-stimulated $[Ca^{2+}]_i$ elevation in the PHN (grey trace) and midpiece (black trace) of a 5 μM 2-APB pre-treated cell. 2-APB was added at the first arrow, 3 μM progesterone at the second arrow. An inflection in the rising phase of the midpiece trace occurs ~20 s after application of progesterone (arrowhead). (**f**) Progesterone-stimulated $[Ca^{2+}]_i$ elevation in the anterior flagellum (dark grey), PHN (light grey) and midpiece (black) of a 5 μM 2-APB pre-treated cell imaged at 10 Hz. Progesterone was applied at 7 s (arrow). The anterior flagellar response precedes responses in the other two compartments and the rising phase of the midpiece response shows an inflexion ~25 s after onset. (**g**) Image series of the same cell as (**f**), showing the delayed $[Ca^{2+}]_i$ rise in the midpiece. Numbers show time in seconds. Progesterone was applied at 7 s.

($P < 0.02$; nine experiments). $[Ca^{2+}]_i$ oscillations (when present) slowed or stopped for 2–3 min (Figure 6b). $[Ca^{2+}]_i$ then recovered to levels slightly above those seen before application of the

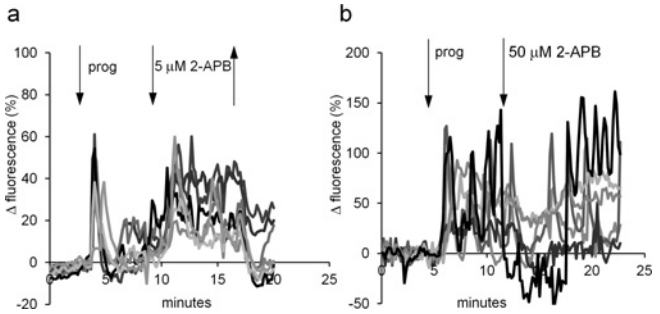

Figure 6 2-APB modifies the sustained $[Ca^{2+}]_i$ elevation

(**a**) 2-APB (5 μM) was applied to cells already stimulated with 3 μM progesterone (prog). 2-APB caused a tonic increase in $[Ca^{2+}]_i$ that reversed upon washout (↑) of the drug. Traces show PHN responses from seven individual representative cells. (**b**) 2-APB (50 μM) was applied to cells already stimulated with 3 μM progesterone. Upon application of the drug, $[Ca^{2+}]_i$ fell and oscillations were suppressed, but $[Ca^{2+}]_i$ then recovered despite the continued presence of the drug. Traces show PHN responses from six individual representative cells.

drug (increment in ΔF_{mean} 4 min after 2-APB $= 5 \pm 2$ %; nine experiments, $P < 0.05$; Figure 6b). 2-APB at 100 μM had a similar effect.

In summary, although the progesterone-induced $[Ca^{2+}]_i$ signal was detectable first in the flagellum, where CatSper is present, pretreatment with 2–5 μM 2-APB 'amplified' the progesterone-induced $[Ca^{2+}]_i$ transient of human sperm at the PHN and midpiece by enhancing activation of a Ca^{2+}-permeable channel that is not CatSper. Pretreatment with high doses of 2-APB (50–100 μM) failed to potentiate the transient and had an inhibitory effect on the sustained $[Ca^{2+}]_i$ increase. Intriguingly, when applied during the $[Ca^{2+}]_i$ plateau, high doses of 2-APB exerted a strong but transient inhibitory action, which was not evident when applied prior to stimulation with progesterone. If 2-APB-sensitive channels contribute to sustained Ca^{2+} influx, inhibition of CatSper by 2-APB (Figure 4d) might release the 2-APB-sensitive channels from inhibitory regulation by $[Ca^{2+}]_i$, leading to recovery of the Ca^{2+} influx.

Orai and STIM proteins are expressed in human sperm

2-APB modulates interaction of STIM with store-operated channel subunits (Orai and possibly TRPC) in the plasma membrane. To investigate STIM and Orai expression in human sperm, we used anti-Orai and anti-STIM antibodies to probe Western blots and to perform immunofluorescent staining.

STIM1

In Western blots, the anti-STIM1 (ProSci catalogue number 4119 and BD Biosciences catalogue number 610954) antibody gave very weak bands. However, after immunoprecipitation with the BD Biosciences antibody, we obtained a strong band at ~95 kDa (Figure 7a), consistent with reports that glycosylation causes the protein to migrate with an apparent mass ⩾90 kDa rather than the predicted 77 kDa [48]. Immunoprecipitation with the Sigma antibody gave a less intense band (results not shown). The positive control [STIM1–GFP (green fluorescent protein) transfected HEK (human embryonic kidney)-293 cells] gave a clear band at ~110 kDa, reflecting the presence of the 25 kDa GFP tag (Figure 7a).

Immunofluorescent staining with the ProSci antibody gave a bright spot at the sperm neck region and also stained the midpiece, which often appeared as two parallel streaks. Antibody

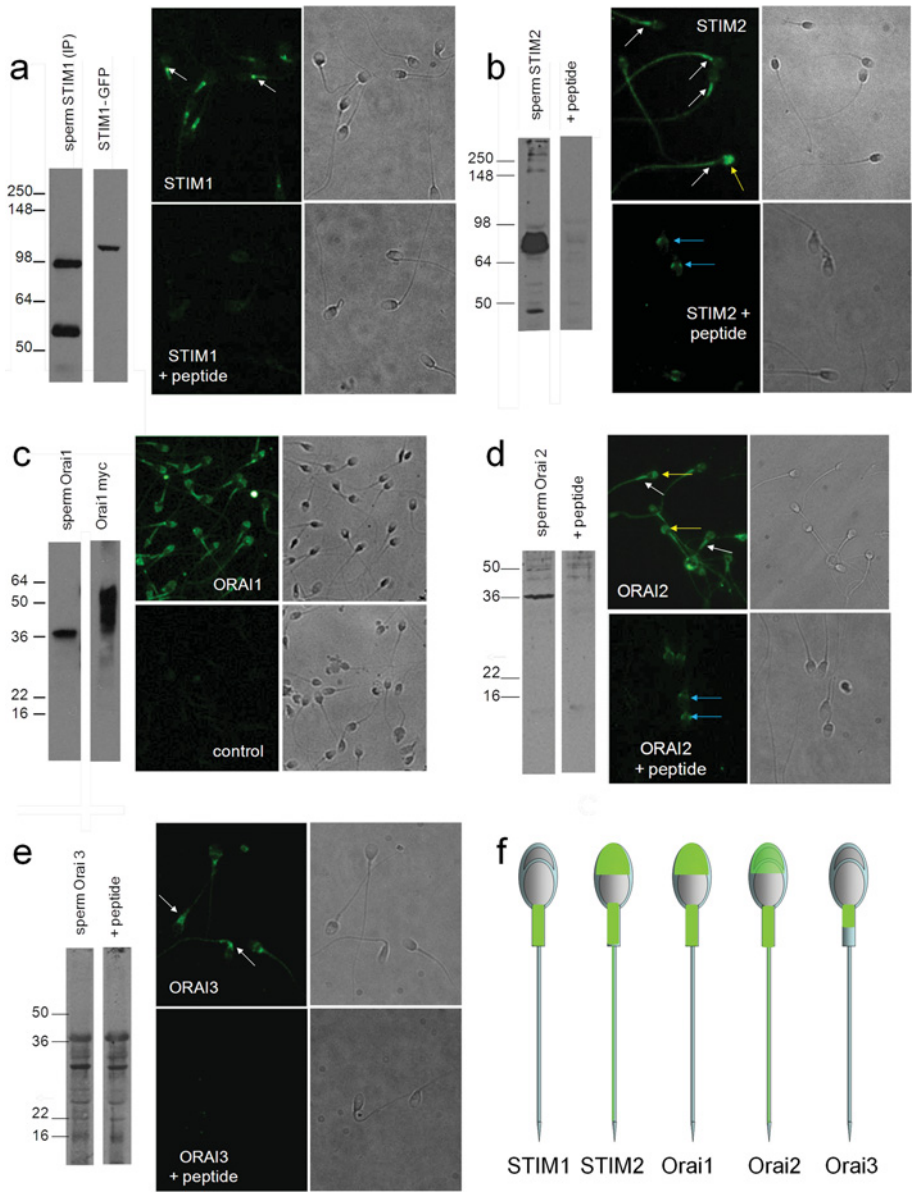

Figure 7 Expression of Orai and STIM in human sperm

(**a**) STIM1. Left-hand panels: Western blot for STIM1 (ProSci 4119); lane 1: human sperm proteins purified by immunoprecipitation with an anti-STIM1 antibody. A band is seen at ∼95 kDa and also at 55–60 kDa due to the presence of anti-STIM1 antibody from the immunoprecipitation procedure. Lane 2 is protein from STIM1–GFP-transfected HEK-293 cells. STIM1 appears at ∼110 kDa due to the presence of the 25 kDa GFP tag. Separation of images in this and other gels indicates that lanes were not originally directly adjacent. Right-hand panels: immunofluorescent staining with anti-STIM1 antibody (ProSci). Upper panels show STIM1 staining and the corresponding phase image. Fluorescence occurs over the midpiece with a bright spot at the sperm neck (arrows). Lower panels show cells incubated with antibody pre-adsorbed with the antigenic peptide, which abolished staining. (**b**) STIM2. Left-hand panels: Western blot for STIM2 (ProSci antibody 4123); lane 1: human sperm proteins. An intense doublet is present at 85–90 kDa. Lane 2: as lane 1, but antibody was pre-adsorbed with the antigenic peptide. Right-hand panels: immunofluorescent staining with anti-STIM2 antibody. The upper panels show STIM2 staining and corresponding phase image. Staining occurs over the flagellum, being heaviest at the midpiece (white arrows). In a minority of cells (<10 %), we observed staining over the acrosome (yellow arrow). The lower panels show cells incubated with antibody pre-adsorbed with the antigenic peptide, which abolished flagellar and acrosomal staining but resulted in fluorescence just behind the equatorial segment (blue arrows). (**c**) Orai 1. Left-hand panels: Orai 1 immunoblot (Sigma antibody O8264); lane 1: human sperm proteins. Lane 2: proteins extracted from Myc-tagged Orai 1-transfected HEK-293 cells. Deduced molecular mass of non-glycosylated Orai 1 is ∼35 kDa. Right-hand panel: immunofluorescent staining with anti-Orai 1 antibody. Upper panels show Orai 1 staining (Sigma antibody O8264) and corresponding phase image. Staining occurs primarily over the acrosome and midpiece and weakly on the principal piece. Lower panels show cells stained similarly but omitting the primary antibody. (**d**) Orai 2. Left-hand panels: Western blot for Orai 2 (ProSci antibody 4111); lane 1: human sperm proteins. Lane 2: as lane 1, but antibody pre-adsorbed with the antigenic peptide. Right-hand panel: immunofluorescent staining with anti-Orai 2 antibody. Upper panels show Orai 2 staining and corresponding phase image. Staining occurs over the midpiece (white arrows) and acrosome (yellow arrows), with weaker staining over the principal piece. Lower panels show cells incubated with antibody pre-adsorbed with the antigenic peptide, which reduces/abolishes staining of the acrosome, midpiece and flagellum, but resulted in fluorescence just behind the equatorial segment (blue arrows). (**e**) Orai 3. Left-hand panels: Western blot for Orai 3 (ProSci antibody 4215). Lane 1: human sperm proteins. Lane 2: as lane 1, but antibody was pre-adsorbed with the antigenic peptide, which did not block band detection. Right-hand panels: immunofluorescent staining with anti-Orai 3 antibody. Upper panels show Orai 3-staining and corresponding phase image. Staining occurs primarily over the anterior midpiece and sperm neck (arrows). Lower panels show cells incubated with antibody pre-adsorbed with the antigenic peptide, which abolished staining. (**f**) Diagrammatic representation of 'typical' localization (immunofluorescence pattern) for each of the proteins investigated.

pre-adsorbtion with the blocking peptide abolished this staining (Figure 7a). Similar localization of STIM1 in human sperm was observed using a different antibody [14].

STIM2

The anti-STIM2 (ProSci catalogue number 4123) antibody gave an intense doublet at 85–90 kDa and a weak band at ≈45 kDa. Pre-adsorption with the blocking peptide abolished this staining (Figure 7b). Immunofluorescent staining occurred on the flagellum, particularly the midpiece. In <10 % of cells we also saw staining over the acrosome (Figure 7b). Antibody pre-adsorption with the blocking peptide completely blocked this staining, but we observed some fluorescence at the equatorial segment that was not seen with unblocked antibody (Figure 7b). The strong STIM2 doublet in the Western blot is consistent with expression of both STIM2 and pre-STIM2 which is cytoplasmic [49], which may explain the surprising finding of staining by anti-STIM2 in the principal piece, where there are no intracellular membranous organelles reported.

Orai 1

In Western blots, anti-Orai 1 (Sigma catalogue number O8264 or ProSci catalogue number 4041) antibody gave a clear band at ∼35 kDa, the predicted mass for the unglycosylated form of the protein. Protein from HEK-293 cells expressing recombinant Myc-tagged Orai 1 (positive control) gave heavy staining between 35 and 50 kDa (Figure 7c), probably reflecting glycosylation [50]. Immunofluorescent staining (Sigma antibody) showed fluorescence over the acrosome and midpiece and weak signal from the principal piece of the flagellum (Figure 7c). Controls without primary antibody gave no significant fluorescence.

Orai 2

Anti-Orai 2 (ProSci catalogue number 4111) gave a strong band of ∼36 kDa in Western blots. The predicted mass is ∼29 kDa, but glycosylation is known to cause Orai migration at higher than predicted molecular mass on SDS/PAGE. Pre-adsorption with the blocking peptide specifically abolished staining of this band (Figure 7d). Immunostaining gave fluorescence over the midpiece and principal piece that was inhibited by pre-adsorption with blocking peptide but, as with STIM2, some staining of the equatorial segment occurred which was not apparent with unblocked antibody (Figure 7d). Controls with no primary antibody gave no fluorescent signal (results not shown).

Orai 3

Western blotting of sperm lysate with anti-Orai 3 (ProSci catalogue number 4215) gave several bands, including one at the predicted mass of ∼36 kDa. Pre-adsorption with the blocking peptide had no effect. Immunofluorescence with the same antibody showed staining primarily over the anterior midpiece and neck that was abolished by pre-adsorption with the blocking peptide (Figure 7e). Owing to the ambiguous nature of these data, we attempted to detect Orai3 by MS but were not able to do so. Proteins of low abundance that are known to be present in sperm can be difficult to detect by this approach, only ∼1000 proteins have been identified so far out of an estimated 2500–3000 in human sperm [51].

TRPV3 (transient receptor potential vanilloid 3)

2-APB at concentrations <10 μM enhances activity of STIM–Orai. The only non-Orai channel type known to be activated by such doses of 2-APB is TRPV3 [52]. Western blotting of human keratinocyte proteins (positive control) for TRPV3 gave a band of the appropriate molecular mass. TRPV3 could not be detected in human sperm (Supplementary Figure S5 at http://www.BiochemJ.org/bj/448/bj4480189add.htm).

Ca^{2+} store mobilization and distribution of STIM proteins

In somatic cells, Ca^{2+} store mobilization causes redistribution of STIM1 to regions of the endoplasmic reticulum close to the plasmalemma, forming distinct puncta [53]. We used 15 μM bis-phenol, which inhibits both SERCA and the secretory pathway Ca^{2+}-ATPase [42] to activate sperm CCE and investigated the effect on distribution of STIM1. Bis-phenol caused sustained $[Ca^{2+}]_i$ elevation within 4 min ($\Delta F_{mean} = 48.7 \pm 3.4$ %; $n = 17$; Supplementary Figure S6a at http://www.BiochemJ.org/bj/448/bj4480189add.htm), an effect that was abolished in EGTA-buffered saline ($[Ca^{2+}] \approx 3 \times 10^{-7}$ M). Application of Ca^{2+} (1.8 mM) to cells treated with bis-phenol in Ca^{2+}-free conditions caused a large sustained $[Ca^{2+}]_i$ elevation, consistent with activation of CCE (Supplementary Figure S6b). We exposed sperm to 15 μM bis-phenol (12 min) in sEBSS, stained for STIM1 and assessed fluorescence in the midpiece as a percentage of the total. In control cells, 60–70 % of total fluorescence was present in the neck/midpiece (Supplementary Figure S6c). Exposure to bis-phenol caused no change ($P > 0.05$; three experiments, 170 cells).

The localization of STIM and Orai primarily to the neck, midpiece and acrosomal regions (Figure 7f) coincides with the locations of Ca^{2+} stores in mammalian sperm [54,55]. TRPC proteins in sperm are also present in these regions [56] and may combine with Orai to form store-regulated or receptor-operated channels [18]. Low concentrations of 2-APB facilitate STIM–Orai interaction [21–23] and the 2-APB-enhanced $[Ca^{2+}]_i$ signalling described above is localized to the PHN. We propose that 2–5 μM 2-APB enhances progesterone-induced Ca^{2+} influx by modulating the activation by STIM of channels incorporating Orai. The presence of STIM2, pre-STIM2 and (potentially) Orai 3 may explain the ability of 2-APB to induce Ca^{2+} influx in the absence of progesterone stimulation and even at doses ⩾50 μM. The mechanism by which progesterone activates these 2-APB-sensitive channels is not yet established. Although activation of Ca^{2+} influx by treatments that mobilize stored Ca^{2+} has been reported on numerous occasions [54] (Supplementary Figure S6b), we were not able to detect conventional CCE currents in human sperm held under conventional whole-cell clamp (results not shown).

Effects of loperamide on progesterone-induced $[Ca^{2+}]_i$ and sperm motility

Loperamide (3–30 μM) is an agonist of SOCs, increasing the Ca^{2+} influx upon store depletion [57]. Loperamide at 10 μM increased resting $[Ca^{2+}]_i$ in 66 ± 7 % of cells ($n = 8$ experiments; Figure 8a). The ΔF_{mean} 90 s after application of loperamide was 24 ± 4 %, increasing to 31 ± 7 % after 3 min ($n = 8$). Superfusion with EGTA-buffered saline (∼3×10^{-7} M) for 3 min prior to loperamide application abolished this effect (results not shown). The cytoplasmic alkalinizing effect of 10 μM loperamide was negligible (0.013 ± 0.005 units; $n = 3$). Inward monovalent

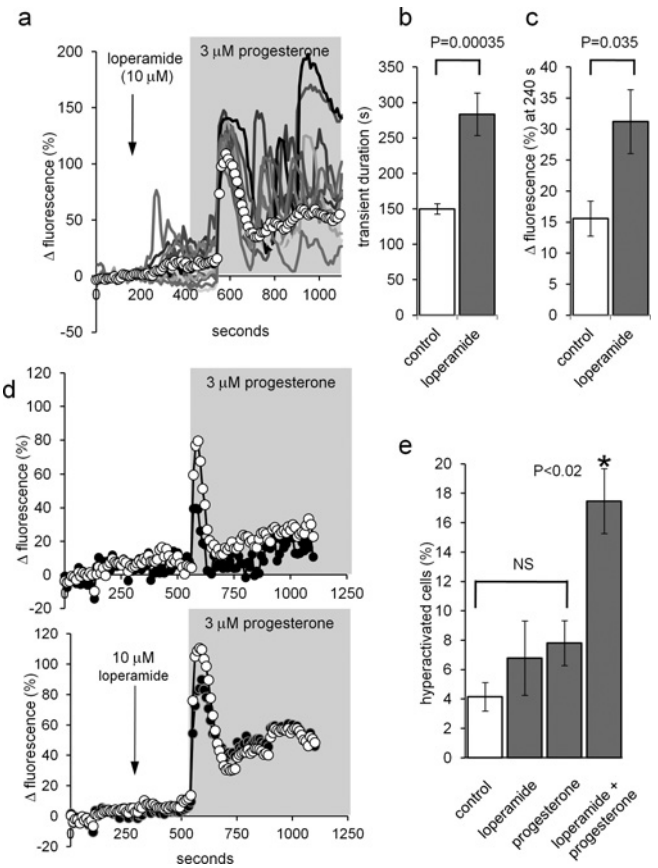

Figure 8 Loperamide potentiates the response of human sperm to progesterone

(**a**) Pre-treatment with 10 μM loperamide (arrow) followed by application of 3 μM progesterone (shading). Traces show nine representative single-cell PHN responses and ΔF_{mean} (○-○) for all 81 cells in the experiment. Loperamide elevates resting $[Ca^{2+}]_i$ and subsequent exposure to progesterone induced an initial $[Ca^{2+}]_i$ transient followed by large $[Ca^{2+}]_i$ oscillations. (**b**) Duration of the progesterone-induced $[Ca^{2+}]_i$ transient in the PHN was increased by loperamide pre-treatment. Bars show means $\pm$ S.E.M. for 11 paired experiments. (**c**) Progesterone-induced sustained $[Ca^{2+}]_i$ increase (ΔF_{mean} at 240 s after progesterone) was enhanced by loperamide pre-treatment. Bars show means $\pm$ S.E.M. for nine paired experiments. (**d**) Mean normalized fluorescence (ΔF_{mean}) in the PHN (○-○) and in the midpiece (●-●) under control conditions (upper panel; mean of 19 cells) and after pre-treatment with 10 μM loperamide (lower panel; mean of 33 cells). Potentiation by loperamide of $[Ca^{2+}]_i$ transient duration and sustained $[Ca^{2+}]_i$ elevation are similar in the two compartments. (**e**) Loperamide enhances progesterone-induced hyperactivation. Each bar shows the percentage of hyperactivated cells (means $\pm$ S.E.M.; $n = 7$). Progesterone (3 μM) and loperamide (10 μM), applied individually, failed significantly to increase hyperactivation (not significant; NS). When cells were pre-treated with loperamide (3 min), progesterone significantly increased the proportion of hyperactivated cells over all the other conditions (*$P < 0.02$).

CatSper currents were insensitive to loperamide and outward currents were semi-reversibly inhibited (Supplementary Figure S7 at http://www.BiochemJ.org/bj/448/bj4480189add.htm).

Effects of 10 μM loperamide on the amplitude of the progesterone-induced $[Ca^{2+}]_i$ transient were inconsistent ($P = 0.38$, paired t test). However, duration of the progesterone-induced $[Ca^{2+}]_i$ transient (ΔF_{mean} initiation to end of falling phase) was significantly increased, from 150 ± 8 to 284 ± 30 s ($P = 0.00035$; paired t test; $n = 11$; Figure 8b). In 10–20 % of cells, the transient peak persisted for 50–100 s and the $[Ca^{2+}]_i$ transient was often followed by a second large plateau or a series of $[Ca^{2+}]_i$ oscillations (Figure 8a). Similarly to pre-treatment with 5 μM 2-APB, an inflexion occurred in the rising phase of the midpiece response in >20 % of cells, indicating activation of the late sustained component of the response. Sustained $[Ca^{2+}]_i$ elevation (ΔF_{mean} 240 s after progesterone) was enhanced ($P < 0.05$; paired t test; $n = 9$) at both the PHN and midpiece (Figures 8c and 8d).

Application of progesterone to free swimming sperm, by mixing or uncaging, induces a burst of transitional or hyperactivated motility, probably associated with the consequent Ca^{2+} transient [58,59], but this rapidly decays, such that effects recorded by CASA are small. Since loperamide pre-treatment both prolongs the $[Ca^{2+}]_i$ transient and enhances the sustained phase, we investigated the effects of loperamide on progesterone-induced hyperactivation. Progesterone (3 μM) alone increased the proportion of cells classified as hyperactivated from 4.2 ± 1.0 to just 7.8 ± 1.5 ($P < 0.01$) and 10 μM loperamide had no significant effect ($P > 0.05$; paired t test, $n = 7$ experiments; Figure 8e). However, when cells were exposed to loperamide for 200 s, then progesterone was applied before introduction into the chamber, the proportion of hyperactivated cells increased to 17.5 ± 2.2 %, significantly greater than progesterone or loperamide exposure alone (Figure 8e; $P = 0.02$; paired t test, $n = 7$ experiments). The loperamide-enhanced sustained $[Ca^{2+}]_i$ signal powerfully modifies motility in human sperm.

Effective progesterone-induced $[Ca^{2+}]_i$ signalling is characteristic of fertile human sperm [9,10]. Our understanding of this non-genomic action of progesterone has recently been transformed by the discovery that CatSper channels in the flagellum of patch-clamped human sperm are activated by this steroid. We have shown in the present study that Ca^{2+}-permeable channels at the sperm neck region, sensitive to 2-APB and loperamide, amplify and prolong progesterone-induced Ca^{2+} signals initiated in the anterior flagellum. Subcellular localization of the Ca^{2+} signal, patch-clamp measurements of CatSper currents and assessment of pH_i confirm that these effects are not by direct or indirect activation of CatSper channels and occur under conditions where CatSper may be partially inhibited. STIM and Orai proteins, which are sensitive to and can be directly activated by low doses of 2-APB, are localized primarily at the sperm neck. We propose that 2-APB-sensitive channels at the sperm neck (probably STIM-regulated Orai or TRPCs) are essential for human sperm Ca^{2+} signalling activated through CatSper, providing amplification, spatio-temporal complexity and flexibility to the sperm Ca^{2+}-signalling toolkit. Release of stored Ca^{2+} and CCE may underly this propagation from the flagellum into the sperm neck region, but we were unable to detect conventional CCE currents in human sperm, so the mechanism of activation of these channels remains an open question.

AUTHOR CONTRIBUTION

Linda Lefièvre, Katherine Nash, Steven Mansell, Sarah Costello, Emma Punt, Joao Correia and Jennifer Morris performed the experimental work. Linda Lefièvre, Katherine Nash, Steven Mansell, Joao Correia, Jackson Kirkman-Brown, Jennifer Morris, Stuart Wilson, Christopher Barratt and Stephen Publicover designed experiments and analysed the data. Stephen Publicover and Christopher Barratt wrote the paper.

ACKNOWLEDGEMENTS

We thank Yuriy Kirichok and Polina Lishko for sharing their sperm-patching expertise, Mike Tomlinson (School of Biosciences, University of Birmingham, Birmingham, U.K.) for Orai1- and STIM1–GFP-expressing cells and Neil Hotchin (School of Biosciences, University of Birmingham, Birmingham, U.K.) for keratinocyte protein extracts.

FUNDING

This work was supported by the Wellcome Trust [grant number 086470] and studentships from the Biotechnology and Biological Sciences Research Council (to K.N. and E.P.) and the Infertility Research Trust (to S.M.).

REFERENCES

1 Publicover, S., Harper, C. V. and Barratt, C. (2007) $[Ca^{2+}]i$ signalling in sperm–making the most of what you've got. Nat. Cell Biol. **9**, 235–242
2 Kirichok, Y. and Lishko, P. V. (2011) Rediscovering sperm ion channels with the patch-clamp technique. Mol. Hum. Reprod. **17**, 478–499
3 Lishko, P. V., Kirichok, Y., Ren, D., Navarro, B., Chung, J. J. and Clapham, D. E. (2012) The control of male fertility by spermatozoan ion channels. Annu. Rev. Physiol. **74**, 453–475
4 Brenker, C., Goodwin, N., Weyand, I., Kashikar, N. D., Naruse, M., Krahling, M., Muller, A., Kaupp, U. B. and Strunker, T. (2012) The CatSper channel: a polymodal chemosensor in human sperm. EMBO J. **31**, 1654–1665
5 Ren, D. and Xia, J. (2010) Calcium signaling through CatSper channels in mammalian fertilization. Physiology (Bethesda) **25**, 165–175
6 Baldi, E., Luconi, M., Muratori, M., Marchiani, S., Tamburrino, L. and Forti, G. (2009) Nongenomic activation of spermatozoa by steroid hormones: facts and fictions. Mol. Cell. Endocrinol. **308**, 39–46
7 Thomas, P. and Meizel, S. (1988) An influx of extracellular calcium is required for initiation of the human sperm acrosome reaction induced by human follicular fluid. Gamete Res. **20**, 397–411
8 Blackmore, P. F., Beebe, S. J., Danforth, D. R. and Alexander, N. (1990) Progesterone and 17 α-hydroxyprogesterone. Novel stimulators of calcium influx in human sperm. J. Biol. Chem. **265**, 1376–1380
9 Krausz, C., Bonaccorsi, L., Maggio, P., Luconi, M., Criscuoli, L., Fuzzi, B., Pellegrini, S., Forti, G. and Baldi, E. (1996) Two functional assays of sperm responsiveness to progesterone and their predictive values in *in-vitro* fertilization. Hum. Reprod. **11**, 1661–1667
10 Forti, G., Baldi, E., Krausz, C., Luconi, M., Bonaccorsi, L., Maggi, M., Bassi, F. and Scarselli, G. (1999) Effects of progesterone on human spermatozoa: clinical implications. Ann. Endocrinol. (Paris) **60**, 107–110
11 Lishko, P. V., Botchkina, I. L. and Kirichok, Y. (2011) Progesterone activates the principal Ca^{2+} channel of human sperm. Nature **471**, 387–391
12 Strunker, T., Goodwin, N., Brenker, C., Kashikar, N. D., Weyand, I., Seifert, R. and Kaupp, U. B. (2011) The CatSper channel mediates progesterone-induced Ca^{2+} influx in human sperm. Nature **471**, 382–386
13 Blackmore, P. F. (1993) Thapsigargin elevates and potentiates the ability of progesterone to increase intracellular free calcium in human sperm: possible role of perinuclear calcium. Cell Calcium **14**, 53–60
14 Park, K. H., Kim, B. J., Kang, J., Nam, T. S., Lim, J. M., Kim, H. T., Park, J. K., Kim, Y. G., Chae, S. W. and Kim, U. H. (2011) Ca^{2+} signaling tools acquired from prostasomes are required for progesterone-induced sperm motility. Sci. Signaling **4**, ra31
15 Putney, J. W. (2009) Capacitative calcium entry: from concept to molecules. Immunol. Rev. **231**, 10–22
16 Cahalan, M. D. (2009) STIMulating store-operated Ca^{2+} entry. Nat. Cell Biol. **11**, 669–677
17 Yuan, J. P., Zeng, W., Huang, G. N., Worley, P. F. and Muallem, S. (2007) STIM1 heteromultimerizes TRPC channels to determine their function as store-operated channels. Nat. Cell Biol. **9**, 636–645
18 Liao, Y., Plummer, N. W., George, M. D., Abramowitz, J., Zhu, M. X. and Birnbaumer, L. (2009) A role for Orai in TRPC-mediated Ca^{2+} entry suggests that a TRPC:Orai complex may mediate store and receptor operated Ca^{2+} entry. Proc. Natl. Acad. Sci. U.S.A. **106**, 3202–3206
19 Cheng, K. T., Liu, X., Ong, H. L. and Ambudkar, I. S. (2008) Functional requirement for Orai1 in store-operated TRPC1-STIM1 channels. J. Biol. Chem. **283**, 12935–12940
20 Maruyama, T., Kanaji, T., Nakade, S., Kanno, T. and Mikoshiba, K. (1997) 2APB, 2-aminoethoxydiphenyl borate, a membrane-penetrable modulator of $Ins(1,4,5)P_3$-induced Ca^{2+} release. J. Biochem. **122**, 498–505
21 Wang, Y., Deng, X., Zhou, Y., Hendron, E., Mancarella, S., Ritchie, M. F., Tang, X. D., Baba, Y., Kurosaki, T., Mori, Y. et al. (2009) STIM protein coupling in the activation of Orai channels. Proc. Natl. Acad. Sci. U.S.A. **106**, 7391–7396
22 Navarro-Borelly, L., Somasundaram, A., Yamashita, M., Ren, D., Miller, R. J. and Prakriya, M. (2008) STIM1-Orai1 interactions and Orai1 conformational changes revealed by live-cell FRET microscopy. J. Physiol. **586**, 5383–5401
23 Yamashita, M., Somasundaram, A. and Prakriya, M. (2011) Competitive modulation of Ca^{2+} release-activated Ca^{2+} channel gating by STIM1 and 2-aminoethyldiphenyl borate. J. Biol. Chem. **286**, 9429–9442
24 DeHaven, W. I., Smyth, J. T., Boyles, R. R., Bird, G. S. and Putney, Jr, J. W. (2008) Complex actions of 2-aminoethyldiphenyl borate on store-operated calcium entry. J. Biol. Chem. **283**, 19265–19273
25 Zhang, S. L., Kozak, J. A., Jiang, W., Yeromin, A. V., Chen, J., Yu, Y., Penna, A., Shen, W., Chi, V. and Cahalan, M. D. (2008) Store-dependent and -independent modes regulating Ca^{2+} release-activated Ca^{2+} channel activity of human Orai1 and Orai3. J. Biol. Chem. **283**, 17662–17671
26 Parvez, S., Beck, A., Peinelt, C., Soboloff, J., Lis, A., Monteilh-Zoller, M., Gill, D. L., Fleig, A. and Penner, R. (2008) STIM2 protein mediates distinct store-dependent and store-independent modes of CRAC channel activation. FASEB J. **22**, 752–761
27 Lis, A., Peinelt, C., Beck, A., Parvez, S., Monteilh-Zoller, M., Fleig, A. and Penner, R. (2007) CRACM1, CRACM2, and CRACM3 are store-operated Ca^{2+} channels with distinct functional properties. Curr. Biol. **17**, 794–800
28 Schindl, R., Bergsmann, J., Frischauf, I., Derler, I., Fahrner, M., Muik, M., Fritsch, R., Groschner, K. and Romanin, C. (2008) 2-Aminoethoxydiphenyl borate alters selectivity of Orai3 channels by increasing their pore size. J. Biol. Chem. **283**, 20261–20267
29 Bootman, M. D., Collins, T. J., Mackenzie, L., Roderick, H. L., Berridge, M. J. and Peppiatt, C. M. (2002) 2-Aminoethoxydiphenyl borate (2-APB) is a reliable blocker of store-operated Ca^{2+} entry but an inconsistent inhibitor of $InsP_3$-induced Ca^{2+} release. FASEB J. **16**, 1145–1150
30 Peppiatt, C. M., Collins, T. J., Mackenzie, L., Conway, S. J., Holmes, A. B., Bootman, M. D., Berridge, M. J., Seo, J. T. and Roderick, H. L. (2003) 2-Aminoethoxydiphenyl borate (2-APB) antagonises inositol 1,4,5-trisphosphate-induced calcium release, inhibits calcium pumps and has a use-dependent and slowly reversible action on store-operated calcium entry channels. Cell Calcium **34**, 97–108
31 Bilmen, J. G. and Michelangeli, F. (2002) Inhibition of the type 1 inositol 1,4,5-trisphosphate receptor by 2-aminoethoxydiphenylborate. Cell. Signalling **14**, 955–960
32 Bilmen, J. G., Wootton, L. L., Godfrey, R. E., Smart, O. S. and Michelangeli, F. (2002) Inhibition of SERCA Ca^{2+} pumps by 2-aminoethoxydiphenyl borate (2-APB). 2-APB reduces both Ca^{2+} binding and phosphoryl transfer from ATP, by interfering with the pathway leading to the Ca^{2+}-binding sites. Eur. J. Biochem. **269**, 3678–3687
33 Harper, C. V., Barratt, C. L. and Publicover, S. J. (2004) Stimulation of human spermatozoa with progesterone gradients to simulate approach to the oocyte. Induction of $[Ca^{2+}]_i$ oscillations and cyclical transitions in flagellar beating. J. Biol. Chem. **279**, 46315–46325
34 Lefievre, L., Chen, Y., Conner, S. J., Scott, J. L., Publicover, S. J., Ford, W. C. and Barratt, C. L. (2007) Human spermatozoa contain multiple targets for protein S-nitrosylation: an alternative mechanism of the modulation of sperm function by nitric oxide? Proteomics **7**, 3066–3084
35 Harper, C., Wootton, L., Michelangeli, F., Lefievre, L., Barratt, C. and Publicover, S. (2005) Secretory pathway Ca^{2+}-ATPase (SPCA1) Ca^{2+} pumps, not SERCAs, regulate complex $[Ca^{2+}]_i$ signals in human spermatozoa. J. Cell Sci. **118**, 1673–1685
36 Fraire-Zamora, J. J. and Gonzalez-Martinez, M. T. (2004) Effect of intracellular pH on depolarization-evoked calcium influx in human sperm. Am. J. Physiol. Cell Physiol. **287**, C1688–C1696
37 Moseley, F. L., Jha, K. N., Bjorndahl, L., Brewis, I. A., Publicover, S. J., Barratt, C. L. and Lefievre, L. (2005) Protein tyrosine phosphorylation, hyperactivation and progesterone-induced acrosome reaction are enhanced in IVF media: an effect that is not associated with an increase in protein kinase A activation. Mol. Hum. Reprod. **11**, 523–529
38 Luconi, M., Bonaccorsi, L., Maggi, M., Pecchioli, P., Krausz, C., Forti, G. and Baldi, E. (1998) Identification and characterization of functional nongenomic progesterone receptors on human sperm membrane. J. Clin. Endocrinol. Metab. **83**, 877–885
39 Osman, R. A., Andria, M. L., Jones, A. D. and Meizel, S. (1989) Steroid induced exocytosis: the human sperm acrosome reaction. Biochem. Biophys. Res. Commun. **160**, 828–833
40 Harper, C. V., Kirkman-Brown, J. C., Barratt, C. L. and Publicover, S. J. (2003) Encoding of progesterone stimulus intensity by intracellular $[Ca^{2+}]$ ($[Ca^{2+}]i$) in human spermatozoa. Biochem. J. **372**, 407–417
41 Kirkman-Brown, J. C., Bray, C., Stewart, P. M., Barratt, C. L. and Publicover, S. J. (2000) Biphasic elevation of $[Ca^{2+}]_i$ in individual human spermatozoa exposed to progesterone. Dev. Biol. **222**, 326–335
42 Brown, G. R., Benyon, S. L., Kirk, C. J., Wictome, M., East, J. M., Lee, A. G. and Michelangeli, F. (1994) Characterisation of a novel Ca^{2+} pump inhibitor (bis-phenol) and its effects on intracellular Ca^{2+} mobilization. Biochim. Biophys. Acta **1195**, 252–258
43 Bedu-Addo, K., Barratt, C. L., Kirkman-Brown, J. C. and Publicover, S. J. (2007) Patterns of $[Ca^{2+}]_i$ mobilization and cell response in human spermatozoa exposed to progesterone. Dev. Biol. **302**, 324–332
44 Garcia, M. A. and Meizel, S. (1999) Progesterone-mediated calcium influx and acrosome reaction of human spermatozoa: pharmacological investigation of T-type calcium channels. Biol. Reprod. **60**, 102–109
45 Servin-Vences, M. R., Tatsu, Y., Ando, H., Guerrero, A., Yumoto, N., Darszon, A. and Nishigaki, T. (2012) A caged progesterone analog alters intracellular Ca^{2+} and flagellar bending in human sperm. Reproduction **144**, 101–109
46 Prakriya, M. and Lewis, R. S. (2001) Potentiation and inhibition of Ca^{2+} release-activated Ca^{2+} channels by 2-aminoethyldiphenyl borate (2-APB) occurs independently of IP_3 receptors. J. Physiol. **536**, 3–19

47 Raffaello, A., De Stefani, D. and Rizzuto, R. (2012) The mitochondrial Ca^{2+} uniporter. Cell Calcium **52**, 16–21
48 Manji, S. S., Parker, N. J., Williams, R. T., van Stekelenburg, L., Pearson, R. B., Dziadek, M. and Smith, P. J. (2000) STIM1: a novel phosphoprotein located at the cell surface. Biochim. Biophys. Acta **1481**, 147–155
49 Graham, S. J., Dziadek, M. A. and Johnstone, L. S. (2011) A cytosolic STIM2 preprotein created by signal peptide inefficiency activates ORAI1 in a store-independent manner. J. Biol. Chem. **286**, 16174–16185
50 Gwack, Y., Srikanth, S., Feske, S., Cruz-Guilloty, F., Oh-hora, M., Neems, D. S., Hogan, P. G. and Rao, A. (2007) Biochemical and functional characterization of Orai proteins. J. Biol. Chem. **282**, 16232–16243
51 Baker, M. A. (2011) The 'omics revolution and our understanding of sperm cell biology. Asian J. Androl. **13**, 6–10
52 Chung, M. K., Lee, H., Mizuno, A., Suzuki, M. and Caterina, M. J. (2004) 2-aminoethoxydiphenyl borate activates and sensitizes the heat-gated ion channel TRPV3. J. Neurosci. **24**, 5177–5182
53 Stathopulos, P. B., Zheng, L., Li, G. Y., Plevin, M. J. and Ikura, M. (2008) Structural and mechanistic insights into STIM1-mediated initiation of store-operated calcium entry. Cell **135**, 110–122
54 Costello, S., Michelangeli, F., Nash, K., Lefievre, L., Morris, J., Machado-Oliveira, G., Barratt, C., Kirkman-Brown, J. and Publicover, S. (2009) Ca^{2+} stores in sperm: their identities and functions. Reproduction **138**, 425–437
55 Ho, H. C. and Suarez, S. S. (2001) An inositol 1,4,5-trisphosphate receptor-gated intracellular Ca^{2+} store is involved in regulating sperm hyperactivated motility. Biol. Reprod. **65**, 1606–1615
56 Darszon, A., Sanchez-Cardenas, C., Orta, G., Sanchez-Tusie, A. A., Beltran, C., Lopez-Gonzalez, I., Granados-Gonzalez, G. and Trevino, C. L. (2012) Are TRP channels involved in sperm development and function? Cell Tissue Res. **349**, 749–764
57 Harper, J. L., Shin, Y. and Daly, J. W. (1997) Loperamide: a positive modulator for store-operated calcium channels? Proc. Natl. Acad. Sci. U.S.A. **94**, 14912–14917
58 Gakamsky, A., Armon, L. and Eisenbach, M. (2009) Behavioral response of human spermatozoa to a concentration jump of chemoattractants or intracellular cyclic nucleotides. Hum. Reprod. **24**, 1152–1163
59 Kilic, F., Kashikar, N. D., Schmidt, R., Alvarez, L., Dai, L., Weyand, I., Wiesner, B., Goodwin, N., Hagen, V. and Kaupp, U. B. (2009) Caged progesterone: a new tool for studying rapid nongenomic actions of progesterone. J. Am. Chem. Soc. **131**, 4027–4030

Received 24 February 2012/22 August 2012; accepted 3 September 2012
Published as BJ Immediate Publication 3 September 2012, doi:10.1042/BJ20120339

Biochem. J. (2012) **448**, 189–200 (Printed in Great Britain) doi:10.1042/BJ20120339

multimedia online data

SUPPLEMENTARY ONLINE DATA

2-APB-potentiated channels amplify CatSper-induced Ca^{2+} signals in human sperm

Linda LEFIÈVRE*†, Katherine NASH‡, Steven MANSELL§, Sarah COSTELLO‡, Emma PUNT‡, Joao CORREIA†‡, Jennifer MORRIS‡, Jackson KIRKMAN-BROWN*†, Stuart M. WILSON§, Christopher L. R. BARRATT§ and Stephen PUBLICOVER‡[1]

*Medical School, University of Birmingham, Birmingham, B15 2TT, U.K., †Birmingham Women's Hospital, Birmingham, B15 2TG, U.K., ‡School of Biosciences, University of Birmingham, Birmingham, B15 2TT, U.K., and §Division of Cardiovascular Medicine, Medical Research Institute, Ninewells Hospital University of Dundee, Dundee DD1 9SY, Scotland, U.K.

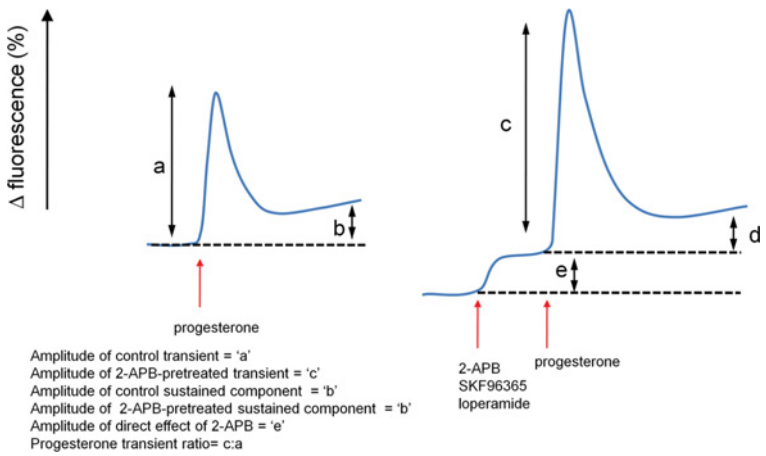

Figure S1 Diagrammatic illustration showing quantified components of $[Ca^{2+}]_i$ traces in control experiments (left) and after pre-treatment with 2-APB (right)

'a' and 'b' show transient and sustained response amplitudes under control conditions. 'c' and 'd' show transient and sustained response amplitudes in 2-APB and loperamide experiments. 'e' shows the amplitude of response to 2-APB or loperamide.

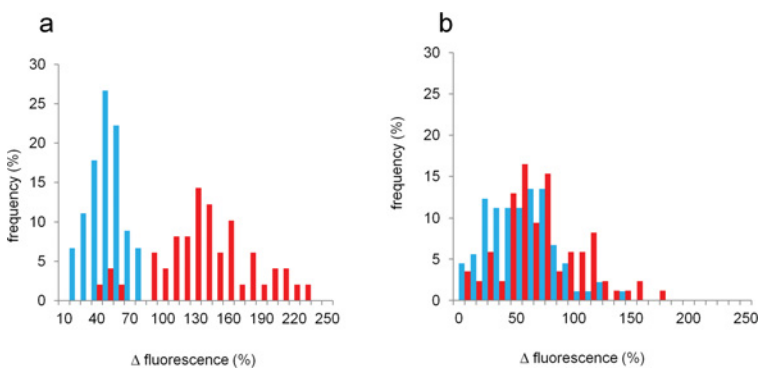

Figure S2 Amplitude distribution for single-cell progesterone transients recorded at the PHN from two pairs of experiments

In each graph, blue bars show the amplitude distribution for the control experiment and red bars show the distribution for a parallel experiment where cells were pre-treated with 5 μM 2-APB. In experiment (**a**), most cells show a large shift to the right after 2-APB pre-treatment but approximately 10 % are clustered at amplitudes similar to the control mean. In experiment (**b**), 2-APB increases the transient amplitude in only a subset of cells, the distribution peak remaining at a ΔF of $\sim$70 %.

[1] To whom correspondence should be addressed (email s.j.publicover@bham.ac.uk

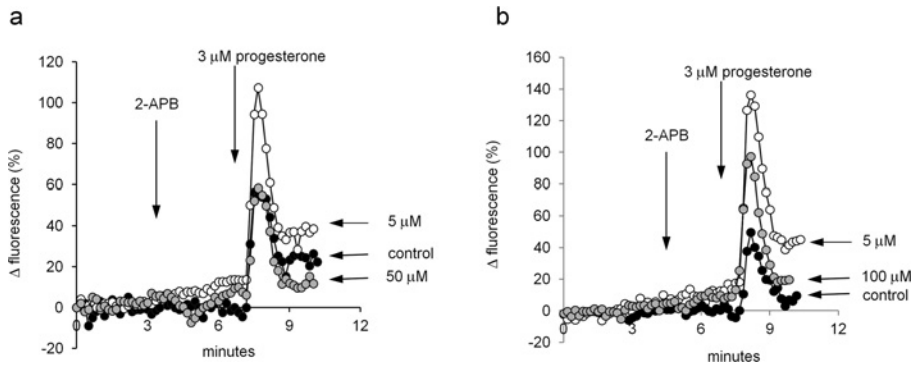

Figure S3 Dose-dependence of effect of pre-treatment with 2-APB on the $[Ca^{2+}]_i$ transient induced by 3 μM progesterone

2-APB (except controls) was added at the first arrow, progesterone (3 μM) was added at the second arrow. (**a**) Black circles, vehicle control; white circles, 5 μM 2-APB; grey circles, 50 μM 2-APB. (**b**) Black circles, vehicle control; white circles, 5 μM 2-APB; grey circles, 100 μM 2-APB.

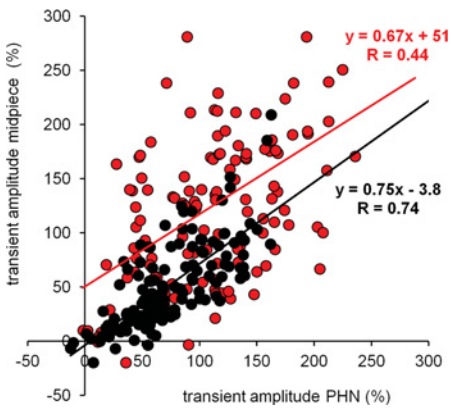

Figure S4 Relationship between the amplitude of the progesterone-induced $[Ca^{2+}]_i$ transient recorded at the PHN (*x* axis) and midpiece (*y* axis)

Under control conditions (black circles), midpiece amplitude is typically $\sim$75 % of amplitude at PHN ($y = 0.75\times - 3.8$). In 5 μM 2-APB-pretreated cells (red circles), both PHN and midpiece transients are larger but also the line of best fit is 'shifted' upward due to recruitment of an extra midpiece component in a sub-population of cells ($y = 0.67\times 51$). The results are from five pairs of experiments; each data set shows $>$130 cells.

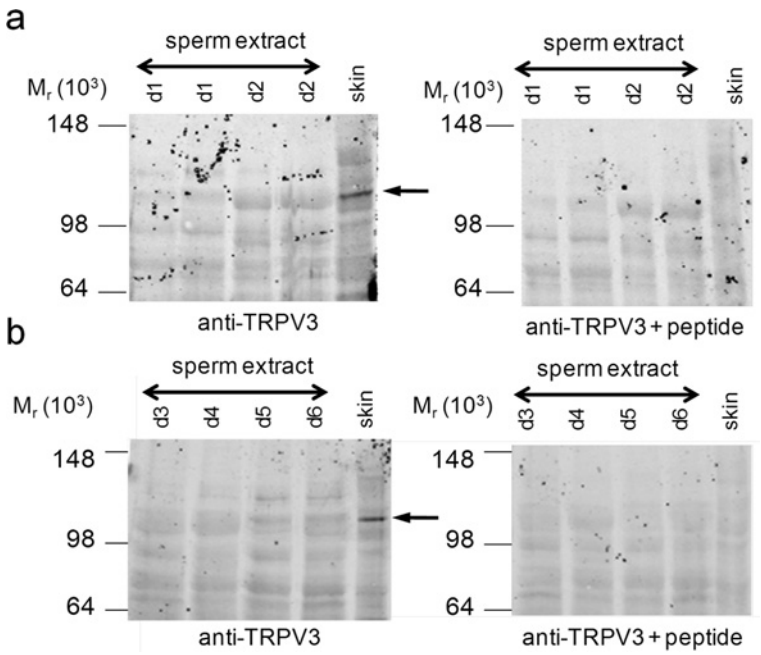

Figure S5 TRPV3 is not detectable in human sperm

(**a**) The left-hand panel shows the immunoblot for TRPV3 with sperm preparations from two different donors (d1 and d2). The final lane shows the positive control (human keratinocyte proteins; skin). The arrow on lane 5 shows the strong band corresponding to the predicted mass for TRPV3. The right-hand panel shows an identical blot, carried out in parallel, after pre-adsorbing the TRPV3 antibody with the antigenic peptide. The band detected in the positive control has been lost. (**b**) As for (**a**), but using four further donors (d3–d6).

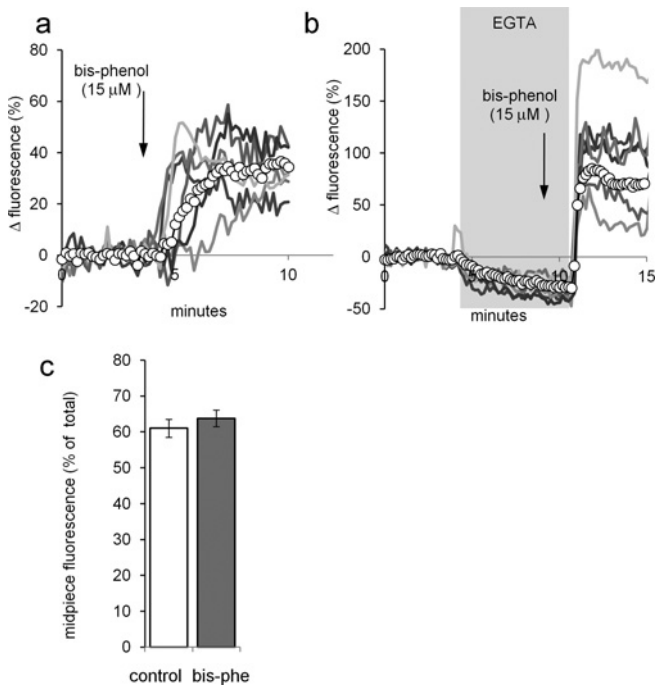

Figure S6 Activation of SOCs does not cause redistribution of STIM1

(**a**) Bis-phenol (15 μM), an inhibitor of Ca^{2+}-store ATPases, causes a sustained increase in $[Ca^{2+}]_i$. Six representative single-cell responses and the means for all cells in the experiment (circles) are shown. (**b**) In EGTA-buffered saline, bis-phenol fails to significantly increase $[Ca^{2+}]_i$, but upon reintroduction of 1.8 mM Ca^{2+}, a large prolonged $[Ca^{2+}]_i$ elevation was seen, indicating the activation of SOCs by store depletion. (**c**) Intensity of immunofluorescent staining of STIM1 in the sperm midpiece (as a proportion of total fluorescence of the sperm) under control conditions (white bar) and after incubation for 12 min in the presence of 15 μM bis-phenol (grey bar). Each bar shows the mean $\pm$ S.E.M. of fluorescence in 170 cells from three experiments.

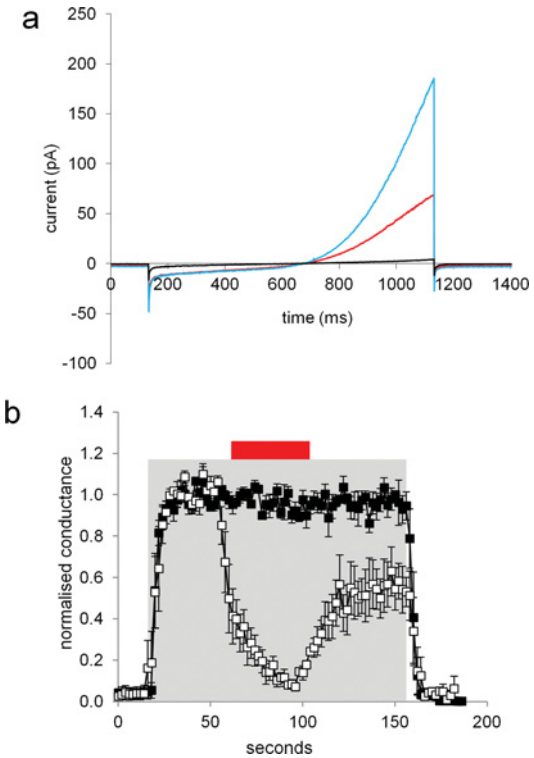

Figure S7 Loperamide does not enhance currents through CatSper channels

(**a**) Currents in a whole-cell clamped sperm induced by a 1 s voltage ramp from -80 mV to $+80$ mV. Black trace shows current in HS medium with 2 mM Ca^{2+} [1]. Blue trace shows current in DVF (divalent cation-free) medium. Red trace shows current in the presence of 10 μM loperamide. (**b**) Time-course of inhibition by 10 μM loperamide of outward conductance (normalized to maximum). Filled squares show control experiments where conductance is reversibly enhanced in DVF medium (shading). Open squares show the effect of 10 μM loperamide (red bar). Each line shows the mean of four experiments $\pm$ S.E.M. Conductance was calculated using $\delta I/\delta V$ at 70–80 mV.

REFERENCE

1 Lishko, P. V., Botchkina, I. L. and Kirichok, Y. (2011) Progesterone activates the principal Ca^{2+} channel of human sperm. Nature **471**, 387–391

Received 24 February 2012/22 August 2012; accepted 3 September 2012
Published as BJ Immediate Publication 3 September 2012, doi:10.1042/BJ20120339